

RESEARCH ARTICLE

Open Access



The remarkable larval morphology of *Rhaebo nasicus* (Werner, 1903) (Amphibia: Anura: Bufonidae) with the erection of a new bufonid genus and insights into the evolution of suctorial tadpoles

Pedro Henrique dos Santos Dias^{1*†}, Jackson R. Phillips^{2†}, Martín O. Pereyra³ , D. Bruce Means^{4,7}, Alexander Haas¹ and Philippe J. R. Kok^{5,6*}

Abstract

Tadpoles serve as crucial evidence for testing systematic and taxonomic hypotheses. Suctorial tadpoles collected in Guyana were initially assigned to *Rhaebo nasicus* through molecular phylogeny. Subsequent analysis of larval and adult morphological traits revealed synapomorphies within the clade encompassing *R. nasicus* and *R. ceratophrys*, prompting the recognition of a new genus described herein as *Adhaerobufo*. The new genus is distinguished from other bufonids by specific phenotypic traits including an enlarged, suctorial oral disc with distinct papillae arrangements, and the presence of certain muscles and narial vacuities at the larval stage. However, only a few adult external characteristics (e.g., enlarged eyelids, infraocular cream spot), seem to be reliably discriminative from related genera. This study underscores the significance of larval morphology in anuran systematics and offers new insights into the evolution of suctorial and gastromyzophorous larvae within bufonids.

Keywords Evolution, Larval traits, Musculoskeletal system, Pantepui, Suctoriality, Systematics, Taxonomy

[†]Pedro Henrique dos Santos Dias and Jackson R. Phillips contributed equally to this work.

*Correspondence:

Pedro Henrique dos Santos Dias
pedrodiasherpeto@gmail.com

Philippe J. R. Kok

philippe.kok@biol.uni.lodz.pl; pjrkok@gmail.com

¹Leibniz Institut zur Analyse des Bioaffiliationswandels, Zoologisches Museum Hamburg, Zentrum für Taxonomie und Morphologie, Martin-Luther-King-Platz 3, 20146 Hamburg, Germany

²Utah State University, 5305 Old Main Hill, Logan, Utah 84322, USA

³CONICET - Agencia INTA General Acha, Avellaneda 530 (8200), General Acha, La Pampa, Argentina

⁴Coastal Plains Institute and Land Conservancy, 1313 Milton Street, Tallahassee, Florida 32303, USA

⁵Department of Ecology and Vertebrate Zoology, Faculty of Biology and Environmental Protection, University of Łódź, 12/16 Banacha Str., Łódź 90-237, Poland

⁶Life Sciences, The Natural History Museum, Cromwell Road, London SW7 5BD, UK

⁷Department of Biological Science, Florida State University, Tallahassee, Florida 32303, USA



© The Author(s) 2024. **Open Access** This article is licensed under a Creative Commons Attribution 4.0 International License, which permits use, sharing, adaptation, distribution and reproduction in any medium or format, as long as you give appropriate credit to the original author(s) and the source, provide a link to the Creative Commons licence, and indicate if changes were made. The images or other third party material in this article are included in the article's Creative Commons licence, unless indicated otherwise in a credit line to the material. If material is not included in the article's Creative Commons licence and your intended use is not permitted by statutory regulation or exceeds the permitted use, you will need to obtain permission directly from the copyright holder. To view a copy of this licence, visit <http://creativecommons.org/licenses/by/4.0/>. The Creative Commons Public Domain Dedication waiver (<http://creativecommons.org/publicdomain/zero/1.0/>) applies to the data made available in this article, unless otherwise stated in a credit line to the data.

Introduction

While adult traits have dominated the field of anuran systematics, biologists have long recognized the potential of larval morphology in better understanding evolutionary relationships. The earliest instance of a larval trait being used in this way can be traced to the late 19th century, when the French zoologist Fernand Lataste [1] proposed a new classification of frogs based on the position of spiracles. A few years earlier, Pizarro [2] had proposed the erection of the genus *Batrachycthis* for the bizarre tadpoles of *Pseudis*. During the following century, the impact of larval morphology on the systematics and taxonomy of anurans was further explored, especially by Noble, who published a series of papers [3–8] advocating the use of larval characters and natural history information in the classification of amphibians. Later, Orton [9] published a seminal paper in which she proposed that four major groups of frogs could be recognized based on larval characters (see also [10]).

Although some authors have argued against the usage of larval characters in taxonomic and systematic studies (e.g., [11, 12]), tadpoles are largely recognized as a source of useful evidence for such studies (e.g., [13–20]). For instance, Haas [21] used larval morphology to propose a new anuran phylogeny that anticipated several phylogenetic trends that have since been supported by the following generation of large-scale molecular studies (e.g., [22–23]).

The past two decades have witnessed constant growth in studies on tadpoles and the exploration of larval characters. Grosjean et al. [24] set a benchmark of the importance of larval characters in systematics, describing a new species based on its tadpole — *Clinotarsus penelope* (Ranidae). Several bizarre and previously unknown larval phenotypes have been described (e.g., [25–32]), and many new characters and synapomorphies for different groups have been proposed (e.g., [33–47]). In the present paper, we discuss the impact of larval morphology on the systematics and taxonomy of a clade of toads of the family Bufonidae.

The true toads, bufonids, are one of the most diverse and speciose anuran clades, with a nearly cosmopolitan distribution (found on all continents except Australia and Antarctica [48]). Currently, the 655 recognized species are allocated in 54 genera [48]. Bufonid diversity is also reflected in their numerous reproductive strategies and developmental modes (e.g., [49–58]). Bufonid tadpoles are also quite diverse, and while many genera have conserved a lentic-benthic larval phenotype (e.g., [59]), there is significant variation in ecology and morphology within the family, including *inter alia* suctorial (sucker mouth) and gastromyzophorous (belly sucker) forms, which represent adaptations to life in fast-flowing waters (e.g., [33, 60, 61]), phytotelma dwellers with endotrophic nutrition

(e.g., [62–64]), open-water species with large, vascular crests [65], semiterrestrial tadpoles that live on wet rocks (e.g., [66]), and direct developers that retain larval traits (e.g., [55]). However, the tadpoles of many bufonid species remain unknown, and while some have assumed that their larval morphology will likely prove to be a typical benthic, lentic form, tadpoles continue to surprise us.

The Pantepui biogeographical region is located in northeastern South America, in the western Guyana Shield highlands, and is famed for its iconic table mountains of Proterozoic sandstone (locally known as “tepuis”). Tepuis are remnants of an enormous landmass (called the Roraima Supergroup or Mataui Formation) resulting from the sedimentation and subsequent uplifts of sandstones produced by the erosion of ancient Gondwanan highlands [67–69]. Over the last two decades a substantial number of new endemic amphibian species (e.g., [70–86], to only cite a few) and even endemic genera and families [87–89] have been described from the region, highlighting the importance of this often neglected biome in the evolution of Neotropical amphibians (see also [90, 91]).

During multiple expeditions in the Eastern Pantepui uplands and highlands of Guyana, DBM and PJRK observed and collected series of brightly colored tadpoles in fast-flowing mountain streams. Until recently, these larvae were assumed to be *Atelopus* cf. *hoogmoedi* based on overall external characteristics and microhabitat (fast-flowing mountain streams). However, a closer examination of the suctorial apparatus and recent molecular phylogenetic analyses indicated that these larvae do not belong to the genus *Atelopus* and should instead be assigned to *Rhaebo nasicus*. As the tadpole of *R. nasicus* is undescribed, we re-examined the larvae of these Pantepui “*Atelopus*” in detail. Our new findings strongly impact the understanding of the taxonomy of these toads and the evolution of bufonid tadpoles more generally.

Materials and methods

Sample determination, molecular data collection and analyses

Species assignment

Adults were assigned to *Rhaebo nasicus* based on external morphology characters, such as the eyelid projection. In Guyana, *R. nasicus* is the only species known to present this character-state. Additional to the phylogenetic placement, the tadpoles were assigned to the family Bufonidae based on the presence of larval synapomorphies of the family: anterolateral process of crista parotica absent, m. diaphragmatopraecordialis absent, lateral fibers of m. subarcualis rectus II–IV invading branchial septum, larval lungs rudimentary, and a single pair of infralabial papillae [21, 33]. In Guyana, there are four genera of bufonids: *Atelopus*, *Oreophrynella*, *Rhaebo*, and *Rhinella*

[48]. All known tadpoles of *Atelopus* present a belly sucker [32], and *Oreophrynella* exhibits endotrophic development [53, 55, 92]. Tadpoles of *Rhaebo guttatus*, *Rhinella marina*, and *R. merianae* have been described [93]. Thus, these tadpoles could only be assigned to *R. nasicus*, *R. beebei*, *R. martyi*, or *R. nattereri* (the three latter being absent from our collection localities).

Tissue sampling, DNA extraction, amplification and sequencing

Genomic DNA was isolated from a small piece of the tail of a preserved tadpole (whole larva fixed in 99% ethanol in the field) from Mount Wokomung, Guyana (CPI10704; 05°00'08"N, 59°52'47"W at 1,573 m elevation) and from liver tissues of two adult *Rhaebo nasicus* (tissues fixed in 99% ethanol in the field) from two localities in Guyana: Kaieteur National Park (IRSNB14518 [PK1348]; 05°08'N, 59°25'W at ca. 540 m elevation), and the slopes of Maringma-tepui (PK1895; 05°12'28"N, 60°33'60"W at 1,060 m elevation).

Tissue samples were digested overnight at 56 °C in a solution of 5 µL of proteinase K and 100 µL of lysis buffer (100 mM NaCl, 100 mM Tris, 25 mM EDTA, 0.5% SDS). DNA extraction was performed using Sera-Mag™ SpeedBeads™ (Thermo Fisher Scientific) at a concentration of ca. 1.7×(105 µl of digested tissue to 180 µL of beads) and eluted into 200 µl of 10 mM Tris buffer. Using polymerase chain reaction (PCR; for primers and PCR conditions see [94]), we amplified a fragment of the barcoding *16S ribosomal RNA gene* (16 S; 507 base pairs [bp]). PCR amplifications were confirmed on a 1% agarose gel, and negative controls were run on all amplifications to exclude contamination. PCR products were purified, and Sanger sequenced (along both strands using the same primers used for PCR) at the Natural History Museum's (NHM, London, UK) sequencing facility. Chromatograms were assembled and edited in Codon-Code Aligner 10.0.2 (Codon Code Cooperation, Dedham, USA). Novel sequences have been catalogued in GenBank (PQ200682–PQ200684). The newly generated sequences were uploaded onto BLAST NCBI (<https://blast.ncbi.nlm.nih.gov/Blast.cgi>) to identify the most similar sequences on GenBank.

Sequences editing and alignment settings

Based on the results of the BLAST analysis and guided primarily by the phylogenetic frameworks established by [95–97], we designed a sampling strategy to determine the placement of the sequenced specimens and elucidate their evolutionary relationships. Accordingly, our phylogenetic analyses focused on a mitochondrial fragment comprising the *12S RNA*, *tRNA valine*, and *16S RNA* genes (*12s-trna-val-16s*), complemented by three nuclear loci: a fragment of the *C-X-C motif chemokine*

receptor 4 gene (*cxc4*), a fragment of the *proopiomelanocortin* gene (*pomc*), and a fragment of the *recombination activating 1* gene (*rag1*) for 82 bufonid specimens and 12 outgroups. Sequences were aligned using MAFFT v7 online software [98–99] with the strategy E-INS-i (for the *12s-trna-val-16s* fragment) and L-INS-i (for remaining fragments). Subsequently, the individual alignments were concatenated using SequenceMatrix v1.8 [100], resulting in a final alignment of 4,668 bp. The brachycephaloid *Ichnocnema guentheri* was used as the outgroup for tree rooting. Details regarding specimens, locality data, and GenBank accession numbers for the sequences used in our analyses are provided in Appendix MS1.

Maximum parsimony phylogenetic analysis

Phylogenetic analysis under Maximum Parsimony (MP) was performed in TNT version 1.6 [101, 102] using “New Technology” searches and treating gaps as a fifth state. The analysis utilized a combination of sectorial searches, ratchet, and tree-fusing techniques [103, 104] until the consensus tree was stabilized 10 times (see [103]). The parameters set of the search were: xmult=replications 10 ratchet 5 drift 5 fuse 5 consense 10. The support for each clade was evaluated by estimating two types of resampling support-measures for the datasets: (1) parsimony jackknife absolute frequencies (JAF; [105]) and (2) parsimony jackknife frequency differences (JGC; [106]). Jackknife supports were estimated performing 1000 replicates using “New Technology” searches with the following settings: xmult=hit 2 replications 12 xss fuse 3.

Maximum likelihood phylogenetic analysis

For Maximum Likelihood (ML) analysis, we initially determined the best partition scheme and corresponding models of nucleotide evolution using ModelFinder [107], as implemented in IQ-TREE 2.2.0 [108] with the command TESTNEWMERGEONLY. Coding genes were partitioned by codon position, while mitochondrial sequences (non-coding) were considered as a single partition. Defined initial partitions are detailed in Appendix MS2.

Subsequently, we searched for the best ML tree in IQ-TREE 2.2.0 with the partition scheme and models of nucleotide evolution selected by ModelFinder. We performed 10 independent searches with different values of perturbation parameter (-pers option) and the tree with the highest likelihood was selected as the optimal tree. For searches we consider edge linked-proportional partition model but separate substitution models and rate evolution between partitions (-spp option). The maximum-likelihood tree was conducted with 1000 ultrafast bootstrap (UFBoot) replicates (-B 1000 option; [109]).

Genetic distances

Uncorrected pairwise distances (UPDs) were calculated in PAUP* [110] for a dataset of the *16S* gene (507 bp, aligned in MAFFT under the

G-INS-i strategy) and containing only sequences of species of *Rhaebo* (see Appendix MS3).

Larval morphology

Larval morphology description is based on four tadpoles in developmental stages 25–38 (*sensu* [111]): three tadpoles (stages 25–26) housed in the National Museum of Natural History, Smithsonian Institution (USNM 592409-11) and one individual (CPI10704) at stage 38 (whose skeleton remains preserved [CPI10704]). All these larvae were originally collected as a single lot (CPI10704) in the Kamana Creek on Mount Kopinang of the Wokomung Massif in Guyana (site MK4; 05°00'08"N, 59°52'47"W at 1,573 m elevation). Terminology for external morphology characters follows [112, 113]. For the study of internal morphology, one tadpole in stage 38 (CPI10704) was submitted to the clearing and double staining protocol of [114]; the process was stopped after the alcian blue step, and the specimen was manually dissected for inspection of larval muscles. After photographic documentation of muscle characters, the palatoquadrate and the hyobranchial skeleton were gently disarticulated; upper and lower jaws were separated and the buccopharyngeal cavity exposed for study of its morphology. After recording characters from muscles and buccopharyngeal cavity, we concluded the clearing process for the study of the larval cranium and hyobranchial morphology. Terminology for the musculoskeletal system follows [47]; buccopharyngeal cavity follows Wassersug [19, 115].

Additionally, one tadpole in Gosner stage 25 (USNM 592409) was stained with phosphotungstic acid [116] and subjected to high-resolution micro-computed tomography (μ CT). The tadpole was μ CT-scanned using a Nikon X TH 225 ST 2x μ CT scanner. Volumetric reconstruction was performed in Nikon CT agent and post-processed in VG Studio Max. Finally, we also examined other tadpoles of different bufonid species (See Appendix MS4).

Adult morphology

We investigated the adult osteology of one individual of *Rhaebo nasicus* housed at the Royal Belgian Institute of Natural Sciences (IRSNB14518) using μ CT scans. The individual was μ CT-scanned using a YXLON FF20 CT. We also μ CT-scanned two adult *R. ceratophrys* (UTA-A4061, UTA-A4062) and two adult *R. haematiticus* (UTA-A57567, UTA-A57572) housed in the herpetological collection of the University of Texas, Arlington, using a Nikon X TH 225 ST 2x μ CT scanner. Some additional species were studied for osteology in (1) cleared and

double stained specimens prepared following the techniques of Wassersug [117] and (2) reconstruction from μ -CT scans (see Appendix MS4).

Evolution of suctoriality

We performed a parsimony optimization of tadpoles' general ecomorphological types in the bufonid tree of life. The evolution of ecomorphological types was assessed using ancestral character state reconstruction as modeled on Fitch's [118] optimization on the Portik et al.'s [97] topology using TNT [101, 102]. Ecomorphological information was taken from Vera Candioti et al. [57].

Results

Phylogenetic analyses and genetic distances

A summary tree of *Rhaebo* and other bufonids is shown in Figs. 1 and 2 (for complete topologies, see MS5 and MS6). The topologies inferred by the MP and ML analyses consistently recover our new sequences within a highly supported clade along with *Rhaebo ceratophrys* and *R. nasicus* (JAF and JGC=100%; UFBoot=100%). The new sequences PQ200683 [IRSNB14518 (PK1348)] and PQ200684 (PK1895) were similar to the only available sequence of *Rhaebo nasicus* in GenBank (DQ158477=ROM20650 [erroneously reported as ROM20560], from Tukeit in Kaieteur National Park, Guyana) with a genetic distance ranging from 0.21 to 0.43%. On the other hand, the sequence PQ200682 (CPI10704) was recovered as the sister lineage of that clade showing a genetic distance ranging from 4.84 to 5.78%. *Rhaebo ceratophrys* is, in turn, sister to the clade composed by the three new sequences and *R. nasicus* ROM20650. In the MP analysis (Fig. 1), the clade *R. ceratophrys*+*R. nasicus* collapses in a polytomy with (1) a moderately well supported clade (JAF=93%, JGC=90%) composed of the remaining included species of *Rhaebo*, (2) the highly supported *Peltophryne* (JAF and JGC=100%) and (3) a moderately well supported clade (JAF=92%, JGC=89%) composed of the "New World" *Anaxyrus*, *Incilius* and *Rhinella*, and all the sampled "Old World" bufonids. In the ML analysis (Fig. 2), the internal topology of the clade *R. ceratophrys*+*R. nasicus* is mostly identical to the MP analysis, nevertheless, the relations of this clade with other bufonids are less conflicting. The clade *R. ceratophrys*+*R. nasicus* is recovered as sister of the remaining *Rhaebo* with high support (UFBoot=98%), and *Rhaebo* is sister to *Peltophryne* with low support (UFBoot=55%). Finally, *Rhaebo*+*Peltophryne* are sister to a well-supported clade (UFBoot=100%) composed of the "New World" *Anaxyrus*, *Incilius*, and *Rhinella*, and all the sampled "Old World" bufonids.

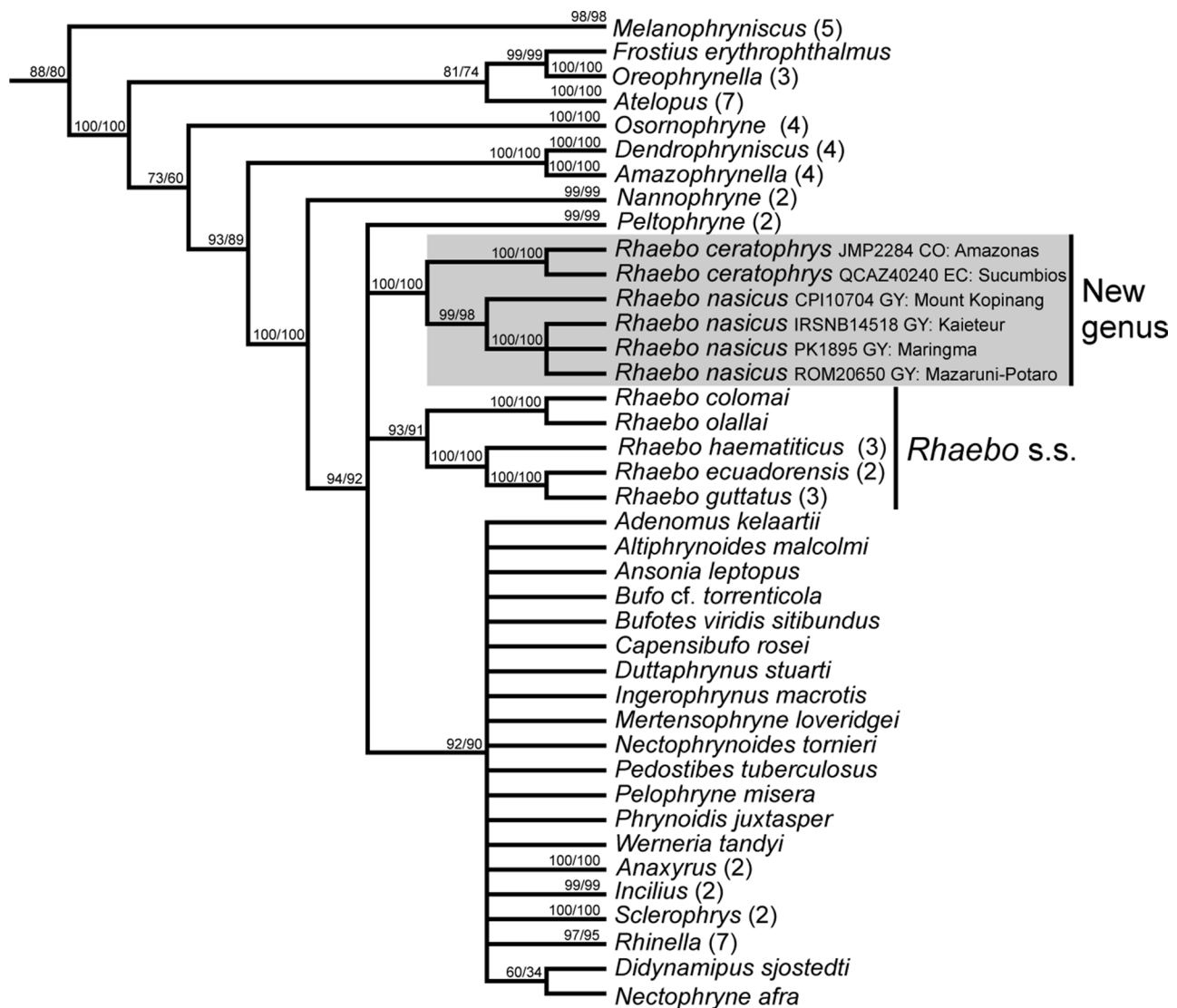


Fig. 1 Summary tree of the maximum parsimony analysis depicting the relationships of *Rhaebo* and other Bufonidae. This tree represents the stabilized strict consensus derived from three most parsimonious trees (of length 15,782 steps). Values at nodes are parsimony jackknife frequencies (absolute/frequency differences). The numbers between parentheses following the names of genera denote the total condensed terminals at that tip. The complete MP strict consensus tree is shown in [MSS](#)

Larval morphology

External morphology (Figs. 3, 4 and 5)

Body compressed (Fig. 3A), elliptical in dorsal (Fig. 3B) and lateral views. Snout rounded in dorsal view, sloped in lateral view. Nostrils positioned dorsofrontally, elliptical, with a medial fleshy projection, anterolaterally directed. Eyes dorsal, laterally directed. Nasolacrimal duct visible (Fig. 3B). Spiracle sinistral, lateral, short, directed posteroventrally; centripetal wall presents as slight ridge. Digestive tract coiled; switchback point laterally dislocated from the center of abdominal region. Vent tube medial, directed posteroventrally, short, distal portion free from ventral fin. Tail higher than body; tail muscle almost reaching tail tip; tail tip rounded. Dorsal and ventral fins convex, about the same height; higher portions

between the middle and posterior thirds of the tail. Dorsal fin originating on the tail. Lateral line system barely visible in preserved material. Oral disc (Fig. 4) enlarged, positioned and directed ventrally, laterally emarginate; a single, continuous row of conical, marginal papillae; no gaps in marginal papillation; submarginal papillae present, in all extension of the lower lip and laterally in the upper lip, with multiple parallel rows. Labial tooth row formula (LTF) 2/3; A1 and A2 length subequal; P2 and P3 length subequal, slightly longer than P1. Jaw sheaths present, serrate, keratinized; upper jaw sheath arch-shaped (slightly less keratinized medially in the photographed specimen); lower jaw sheath V-shaped.

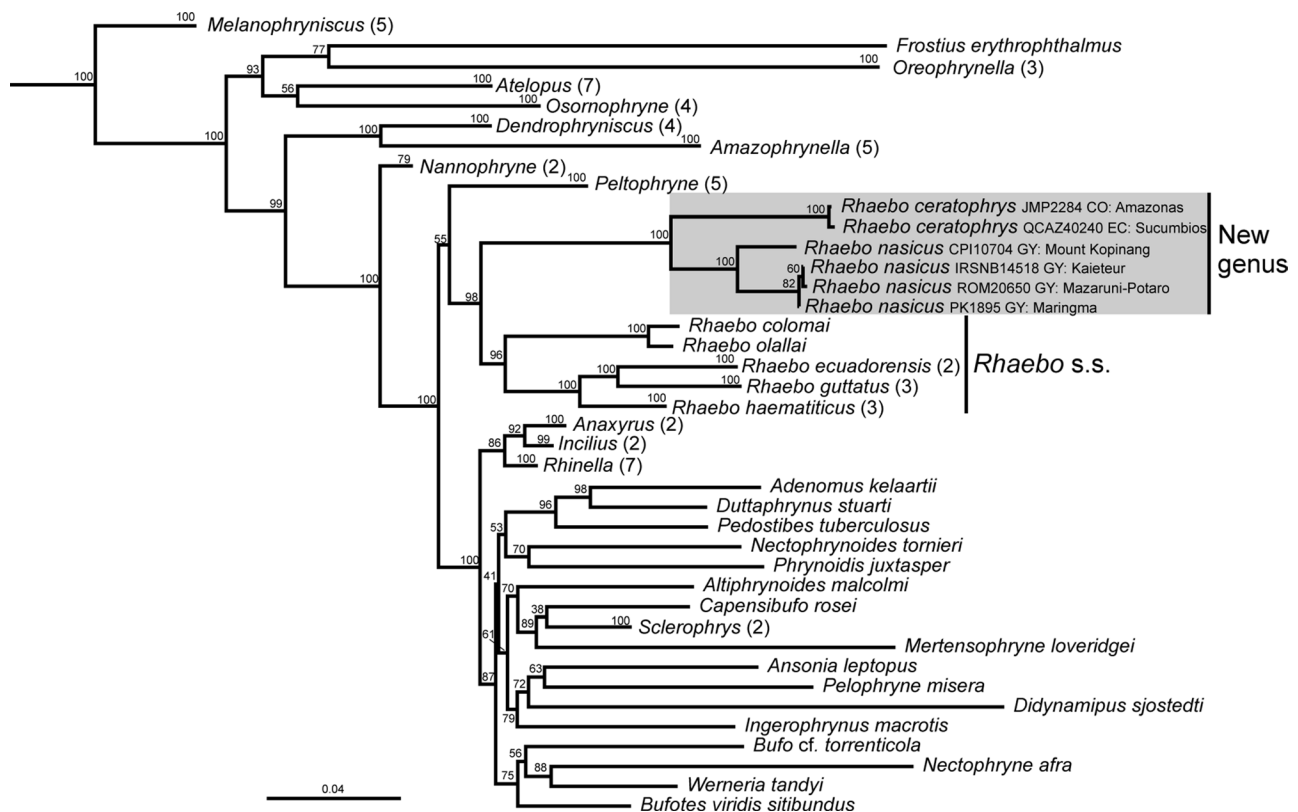


Fig. 2 Summary tree of the maximum likelihood analysis depicting the relationships of *Rhaebo* and other Bufonidae. Values at nodes are bootstrap values. The numbers between parentheses following the names of genera denote the total condensed terminals at that tip. The complete ML tree is shown in MS6

Color in life

In life (Fig. 5), the overall coloration is yellow-gold dorsally and ventrally but is divided into five yellow-gold bands by four transverse dark bands of approximately the same width. The tadpole snout is yellow-gold from the tip to the eye, then the narrowest yellow-gold band encircles the midbody with an overwash of dark pigment. The posterior one-third of the tadpole body is densely black set off by the first of three yellow bands on the tail, the tip of which is the last yellow-gold band. The oral disc is translucent. Ventral views reveal a fading of the dark banding pattern along the body, with translucent skin offering glimpses of internal organs. Upon preservation, the vibrant hues subside, and the yellow-gold bands take on a cream-colored appearance separated by dark brown bands with scattered light brown blotches (Fig. 2).

Buccopharyngeal cavity (Fig. 6)

Buccal roof (Fig. 6A) triangular. Prenarial arena (Fig. 6C) rectangular, with a triangular protuberance. Internal nares elliptical (Fig. 6C), transversally oriented; posterior valve free, with small, triangular projections in the anterior wall. Vacuities present, circumscribed by margins of inner nares. Postnarial arena diamond-shaped, two conical, short postnarial papillae. Lateral ridge papillae

short, trifurcated. Median ridge low, triangular, with a medial notch at its apex. Buccal roof arena poorly delimited, defined by a single pair of conical papillae each side. Glandular zone poorly defined. Dorsal velum medially continuous, devoid of papillae or projections, arch shaped.

Buccal floor (Fig. 6B) triangular. Single pair of flat, wide, branched, infralabial papillae; small papilla-like structures after mouth opening (Fig. 6D). Lingual bud well developed, rounded; lingual papillae absent. Buccal floor arena bell-shaped; 7–8 papillae each side. Buccal floor arena lacking pustulations. Prepocket papillae and pustulation absent. Buccal pockets deep, wide, oblique slit shaped. Ventral velum present; spicular support conspicuous; medial notch absent; secretory pits poorly developed; secretory ridges present. Branchial basket triangular, short, poorly developed, wider than long.

Larval cranium (Fig. 7)

Neurocranium longer than wide; greatest width at the subocular bar level (Fig. 7A–B). Suprarostal cartilage (Fig. 7C) formed by the suprarostal alae and suprarostal corpora; both corpora are medially fused and connected to the proximal region of the triangular alae. An adrostral tissue mass is present close to the posterior process

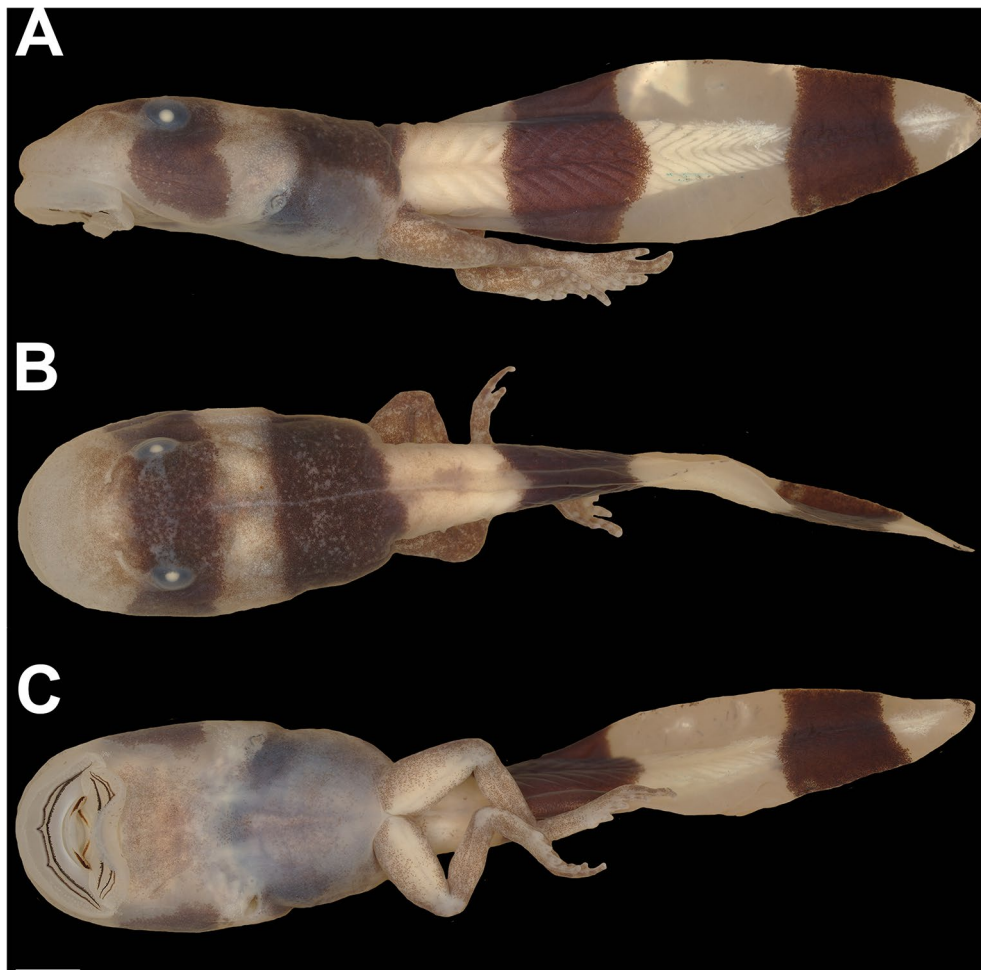


Fig. 3 The tadpole of “*Rhaebo*” *nasicus* (CPI10704) at stage 38 in lateral (A), dorsal (B), and ventral (C) views. Scale bar = 1.0 mm. Photos by Pedro H. Dias

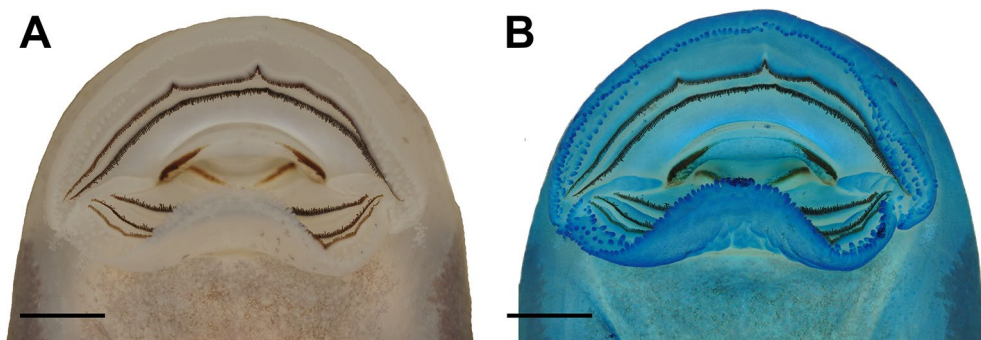


Fig. 4 The oral disc of “*Rhaebo*” *nasicus* (CPI10704) tadpole at stage 38 in natural, preserved coloration (A) and stained with methylene blue to highlight anatomical features (B). Scale bars = 1.0 mm. Photos by Pedro H. Dias

of the alae (Fig. 7C); under dissection, it did not appear to be chondrified, but histological analysis should be done to confirm. Ethmoidal region short; trabecular horns long, diverging in a “V” pattern; trabecular horns greatly expanded anteriorly. Basicranial fenestra weakly chondrified, partially occluded by a thin membrane. Taenia tecti medialis and transversalis present and confluent (Fig. 7A),

dividing the frontoparietal fontanelle in three. Orbital cartilage low. Otic capsules robust, rhomboidal in dorsal view, representing ca. 1/4 of chondrocranium length; synotic tectum connects the two capsules. Palatoquadrate, thin in lateral view, attached to neurocranium through a wide anterior quadratocranial commissure and an almost perpendicular ascending process. Articular process wide.



Fig. 5 Living tadpole of “*Rhaebo*” *nasicus* in right lateral (A), dorsal (B), and ventral (C) views. Photos by D. Bruce Means

Muscular process triangular, well-developed, and curved dorsomedially. Connection between the tip of the muscular process and the neurocranium through a chondrified quadrato-orbital commissure. Palatoquadrate C-shaped, clearly concave; posterior curvature of palatoquadrate reaching the level of the otic capsules.

In the lower jaw (Fig. 7D), Meckel’s cartilage sigmoid, transversely oriented, almost perpendicular to the chondrocranium longitudinal axis. Infracranial cartilages rectangular in frontal view, curved, joined at the symphysis (Fig. 7D).

Ceratohyals (Fig. 7E) long, flat, and subtriangular; anterior margin with well-developed anterior and anterolateral processes; posterior processes triangular and long. Ceratohyals confluent joined by a chondrified pars reuniens. Basibranchial rectangular, with rounded urobranchial process present. Basihyal absent. Hypobranchial plates long, triangular. Branchial basket with four curved ceratobranchials bearing lateral projections. Ceratobranchial I with a triangular anterior branchial process, continuous with the hypobranchial plate. Ceratobranchials II and III joined by the proximal commissure. Four long, curved spicules projecting dorsally from the ceratobranchials. Ceratobranchials distally joined by terminal commissures.

Muscles (Figs. 8, 9 and 10)

We identified 32 muscles (Table 1); most of *Rhaebo nasicus* muscles followed general patterns of origin and

insertion of other bufonids and other anurans (Figs. 8, 9 and 10). Interestingly, the lateral fibers of the subarcualis rectus II–IV invade the interbranchial septum IV (Fig. 9) and the presence of the rectus abdominis anterior.

Visceral components

Digestive tract short; coiled gut with switchback point sinistral. Liver enlarged, occupying a significant portion of the abdominal cavity. Lungs short, inflated, pigmented.

Adult morphology

The adult morphology of both *Rhaebo nasicus* and *R. ceratophrys* has been widely reviewed in the literature, including aspects of their osteology (e.g., [96, 119–121]). The most obvious shared character between *R. nasicus* and *R. ceratophrys* is the presence of an enlarged eyelid in both species (although more distinctly projecting in *R. ceratophrys*). An infraocular cream spot is also evident in adult specimens of both species. Additionally, both species share a narrow sphenethmoid (see below).

Pramuk defined the “*Bufo guttatus* group” (= *Rhaebo*) as presenting two unique, unreversed synapomorphies: the sphenethmoid in ventral view is distinctively broad, and the posterior process of the prootic is prominent and notched ([121]:434). Pramuk did not consider *B. nasicus* to be part of that clade and stressed that *B. nasicus* and the *B. guttatus* group share the presence of a well-developed omosternum and an elongated transverse process of

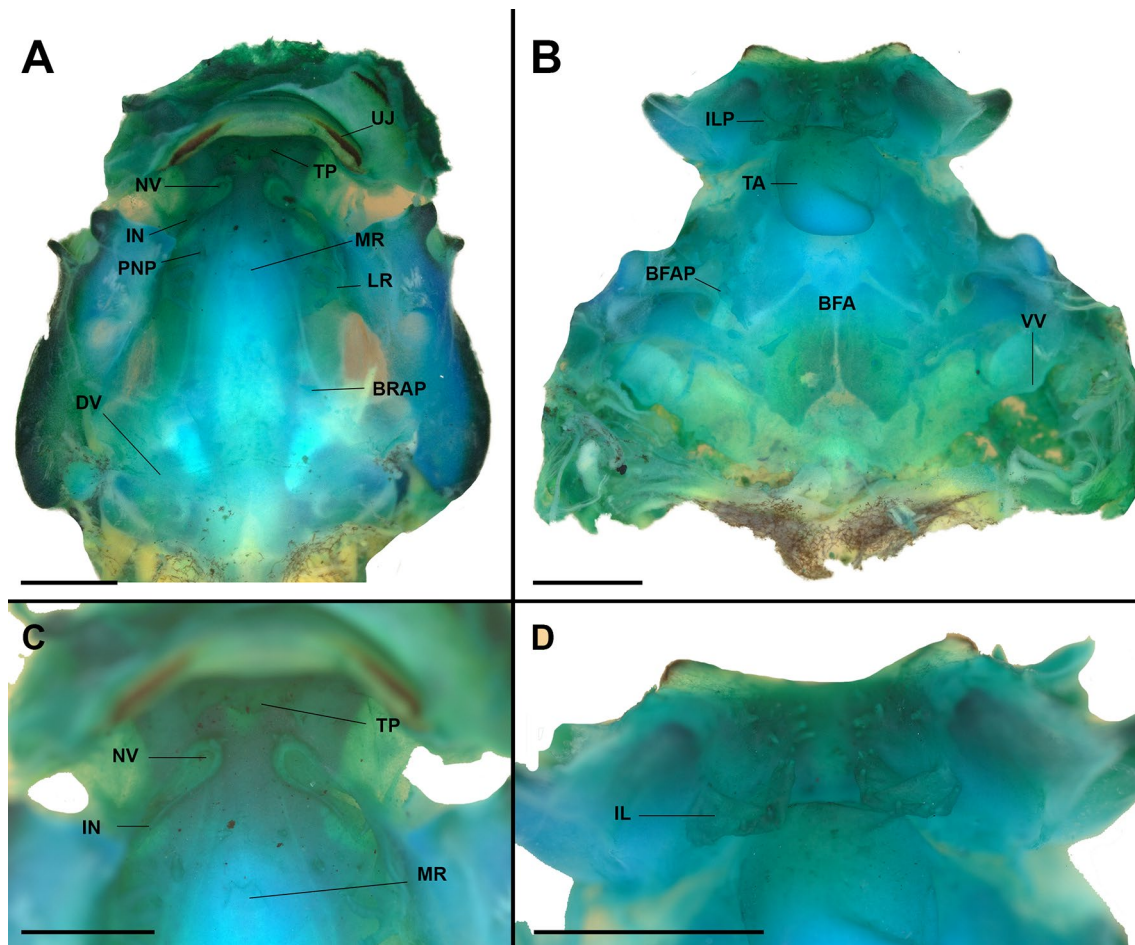


Fig. 6 The buccopharyngeal cavity of “*Rhaebo*” *nasicus* (CPI10704) tadpole at stage 38. Buccal roof (A) and floor (B) morphologies, with details of the pre- and postnarial arenas (C) and of the infralabial and lingual (D) regions. BFA, buccal floor arena; BFAP, buccal floor arena papillae; BRAP, buccal roof arena papillae; DV, dorsal velum; ILP, infralabial papillae; IN, internal nares; LR, lateral ridge; MR, median ridge; NV, narial vacuities; PNP, postnarial arena papillae; TA, tongue anlage; TP, triangular projection; UJ, upper jaw sheath; VV, ventral velum. Scale bars = 1.0 mm. Photos by Pedro H. Dias

vertebra VI ([121]:434). However, most of the osteological characters for *B. nasicus* were missing in her analysis.

Ron et al. ([95]:354) proposed a redefinition for the states “narrow” and “distinctively broad” for the sphenethmoid condition of Pramuk ([121]: ch35), considering the species of *Rhaebo* to have a “wide condition” due to the lateral edges of the sphenethmoid being in contact with the frontoparietals. In species where the frontoparietals do not extend to the anterior portion of the orbit (e.g., *Peltophryne*), a more accurate definition of the “wide” condition of the sphenethmoid could be as follows: the sphenethmoid reaches the margin of the orbit immediately posterior to the palatines. Both “*R. ceratophrys*” and “*R. nasicus*” have a narrow condition of the sphenethmoid (i.e., the sphenethmoid does not reach the margin of the orbit immediately posterior to the palatines), differentiating them from other *Rhaebo* (Fig. 11). The narrow condition of the sphenethmoid is also

observed in bufonids closely related to “*R. ceratophrys*” and “*R. nasicus*”, such as *Amazophrynella*, *Nannophryne* and *Peltophryne*, which suggests the wide sphenethmoid to be a synapomorphy of *Rhaebo* sensu stricto.

Regarding the second synapomorphy of *Rhaebo* proposed by Pramuk ([121]; i.e., posterior process of the prootic prominent and notched), Ron et al. [95] pointed out a perceived error in the identification of the anterior prootic processes (sic) by Pramuk [121], stating that they were, in fact, the occipital condyles, which are part of the exoccipital rather than the prootic. However, both structures are clearly illustrated and identified in Fig. 5A of Pramuk’s work [121], suggesting a possible misunderstanding of these structures by Ron et al. [95], so we follow Pramuk [121]. In this regard, “*R. ceratophrys*” and “*R. nasicus*” have prominent and notched posterior process of the prootic as other species of *Rhaebo*, but also seen in some species of *Peltophryne* ([121]: Fig. 2).

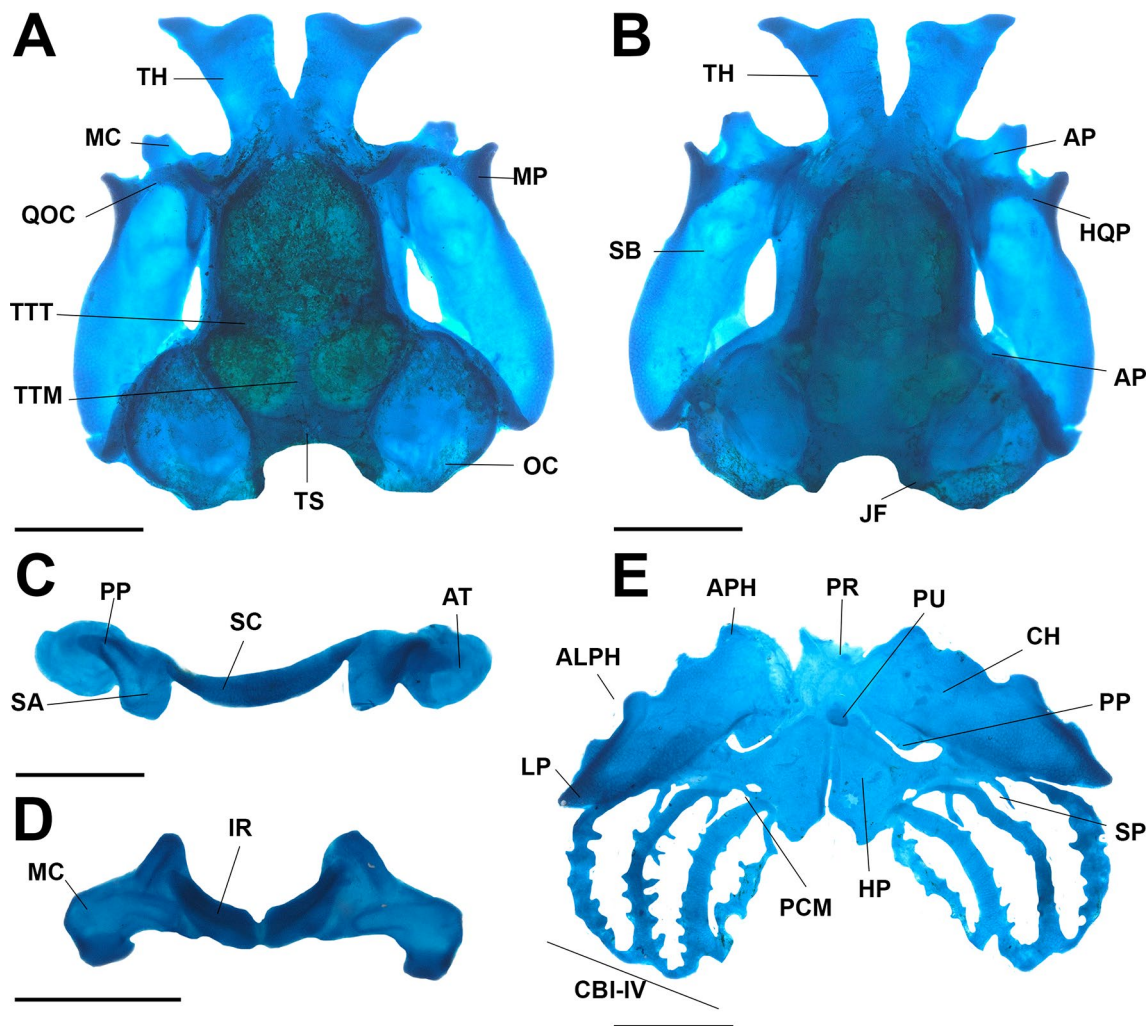


Fig. 7 The larval cranium of “*Rhaebo*” *nasicus* (CPI10704) tadpole at stage 38. Dorsal (A), ventral (B) views, details of the supraorbital (C) and Meckel’s cartilage (D), and hyobranchial apparatus (E). ALPH, antelateral process hyalis; AP, articular process; APH, anterior process hyalis; AT, adrostral tissue; CB, constrictor branchialis; CH, ceratohyal; HP, hypobranchial plate; HQP, hyoquadrate process; IR, infraorbital cartilage; JF, jugular foramen; LP, lateral process; MC, Meckel’s cartilage; MP, muscular process; OC, otic capsule; PCM, proximal commissure; PP, posterior process; PU, process urobranchialis; QOC, quadro-orbital commissure; SA, supraorbital ala; SB, subocular bar; SC, supraorbital copora; SP, spicule; TH, trabecular horns; TS, tectum synoticum; TTM, taenia tecti medialis; TTT, taenia tecti transversalis. Scale bars = 1.0 mm. Photos by: Pedro H. Dias

Comments on the taxonomic and systematic history of “*Rhaebo*” *ceratophrys* and “*Rhaebo*” *nasicus*

Rhaebo ceratophrys was first described in 1882 by Boulenger ([122] as *Bufo ceratophrys*) based on a juvenile specimen from Ecuador (BMNH 1880.12.5.151). The species was characterized by a unique feature, a long eyelid projection. Since then, the species has been transferred to several different species groups within the former genus *Bufo*. For instance, Gallardo [123] allocated it in the *B. marinus* group, whereas Cei [124], Hoogmoed [120] and Pramuk [121] considered the species as belonging to the *B. typhonius/margaritifera* group.

The taxonomic history of *Rhaebo nasicus* has also been convoluted. Werner [125] found a specimen of an unknown toad (IRSNB1015, formerly IRSNB4792),

which he named *Bufo nasicus*. Later, studies of the contents of its digestive tract suggested a South American origin (Smith and Laurent 1950), and eventually Hoogmoed [120] accessed additional specimens from Guyana and Venezuela. He compared these individuals with the redescription and illustrations made by Smith and Laurent [126], identifying them as the *Bufo nasicus* of Werner [125]. Hoogmoed [120] redescribed the species and suggested it to be restricted to the Guiana Shield. Hoogmoed [120] noted the presence of an enlarged eyelid in *B. nasicus* and argued that the shared presence of such an eyelid in *B. nasicus* and in *B. ceratophrys*, as well as similar color patterns indicate a close relationship between the two species. Hoogmoed [120] also noted that *B. ceratophrys* was much smaller than *B. nasicus* — a

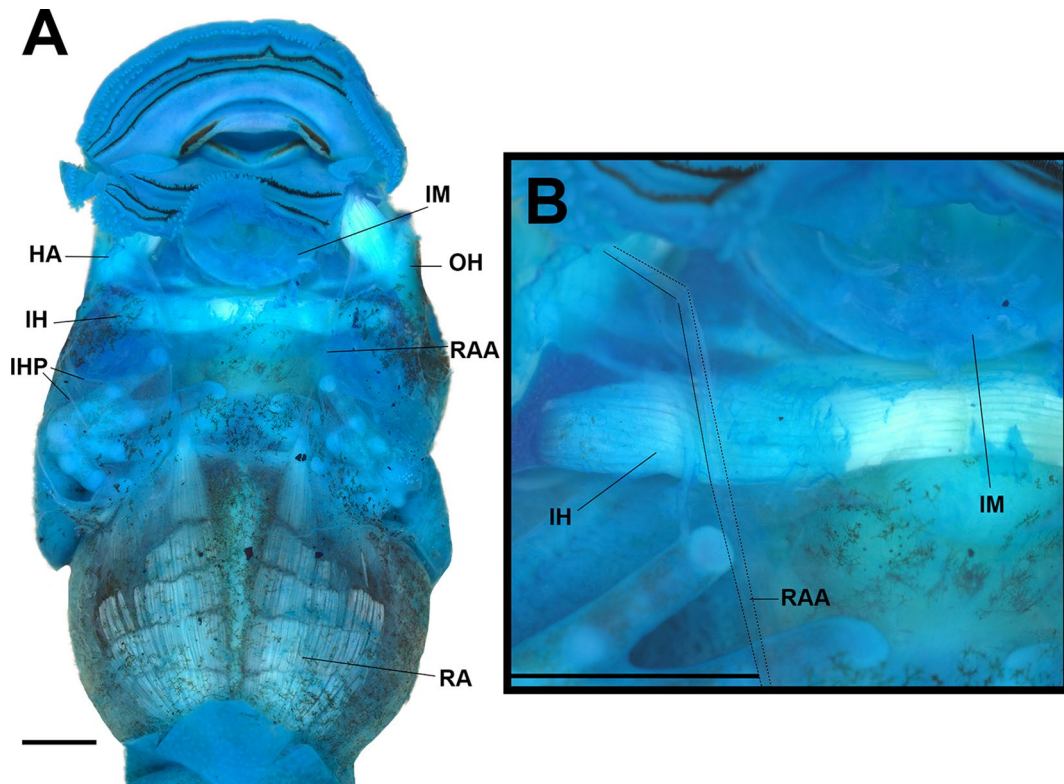


Fig. 8 The larval muscles of *Rhaebo nasicus* (CPI10704) tadpole at stage 38 in ventral view (A); detail of the tendon of the m. rectus abdominis anterior (B). HA, hyoangularis; IH, interhyoideus; IHP, interhyoideus posterior; IM, intermandibularis; OH, orbitohyoideus; RA, rectus abdominis; RAA, rectus abdominis anterior. Scale bars = 1.0 mm. Photos by: Pedro H. Dias

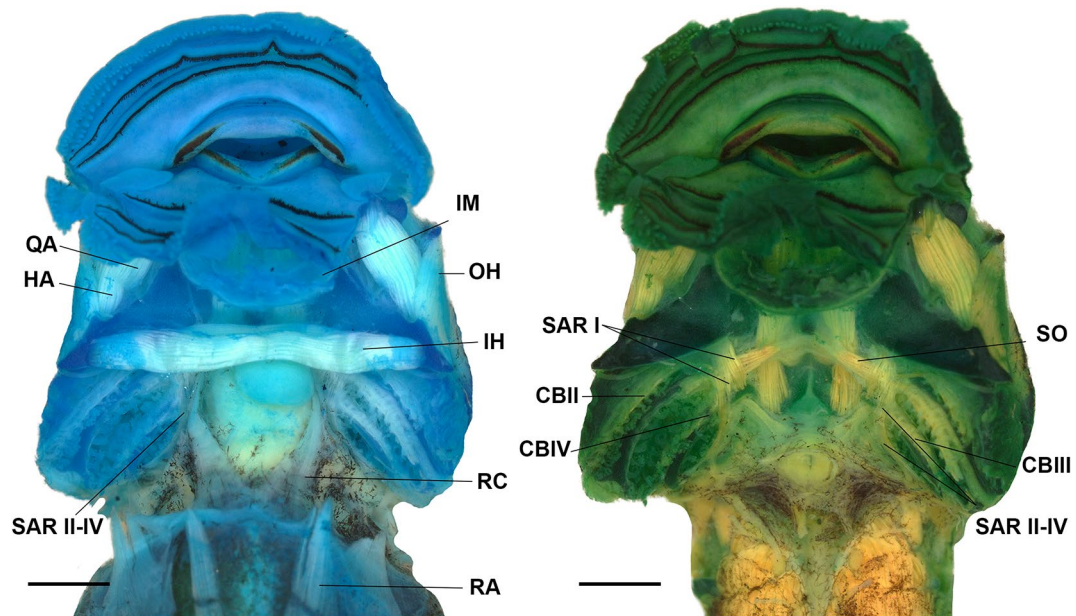


Fig. 9 The larval muscles of *Rhaebo nasicus* (CPI10704) tadpole at stage 38 in ventral view. CB, constrictor branchialis; HA, hyoangularis; IH, interhyoideus; IM, intermandibularis; OH, orbitohyoideus; QA, quadrato-angularis; RA, rectus abdominis; RC, rectus cervicis; SAR I, subarcualis rectus I; SAR II-IV, subarcualis rectus II-IV; SO, subarcualis obliquus. Scale bars = 1.0 mm. Photos by Pedro H. Dias

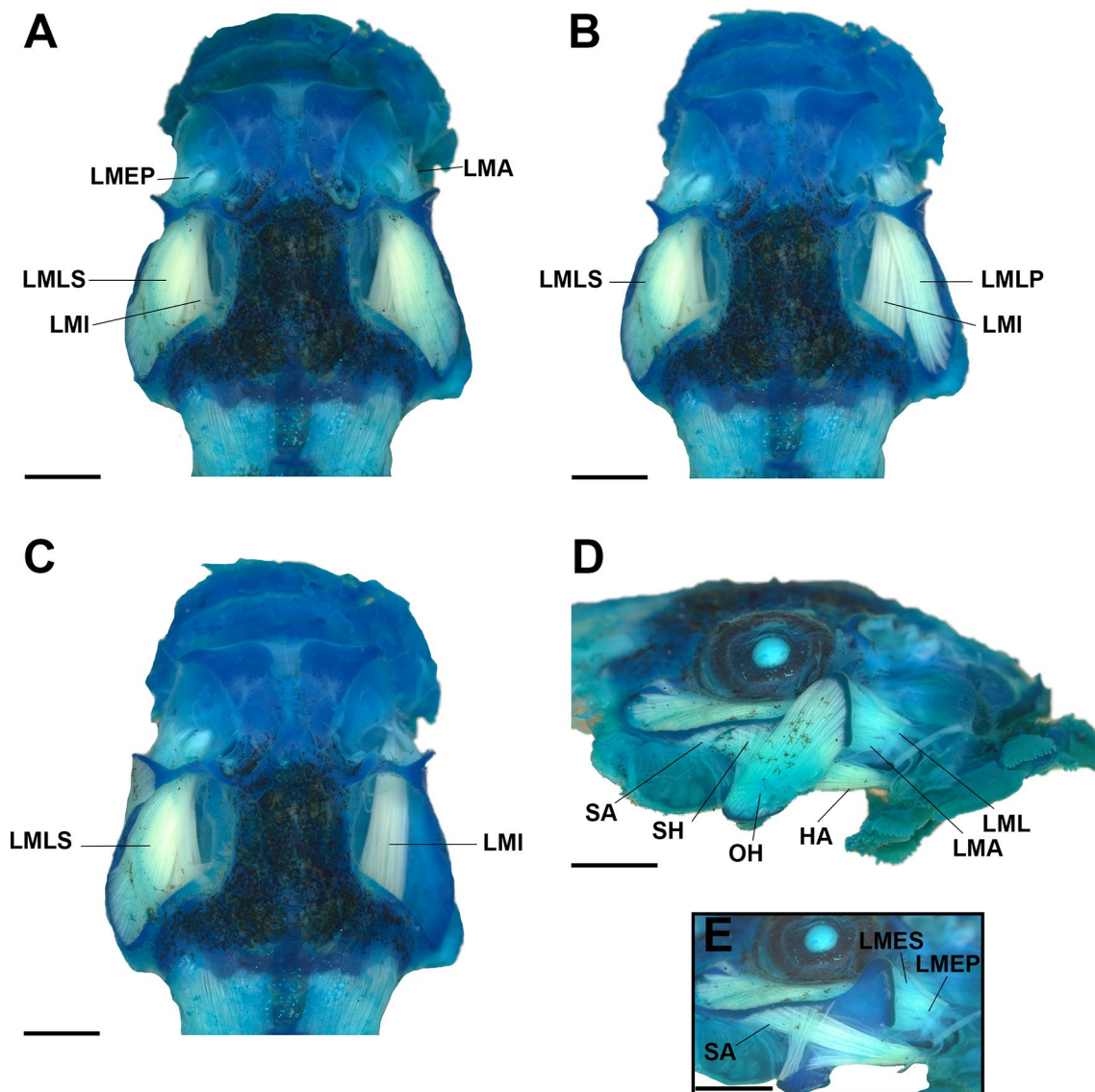


Fig. 10 The larval muscles of “*Rhaebo*” *nasicus* (CPI10704) tadpole at stage 38 in dorsal (A–C) and lateral (D–E) views. LMA, levator mandibulae articularis; LMEP, levator mandibulae externus profundus; LMES, levator mandibulae externus superficialis; LMI, levator mandibulae internus; LMLS, levator mandibulae longus superficialis; OH, orbitohyoideus; SA, suspensorioangularis; SH, suspensoriohyoideus. Scale bars = 1.0 mm. Photos by: Pedro H. Dias

misinterpretation repeated by others (e.g., [127]), since the holotype of *B. ceratophrys* is a juvenile.

Pramuk [121] performed an extensive phylogenetic analysis of Bufonidae, using both morphology and molecular data. She recovered *Bufo nasicus* as sister to other species of the *Bufo guttatus* group of Blair [128] in all analyses (morphological, mitochondrial genes, nuclear genes, and combined analyses). She also examined specimens of *B. ceratophrys* (her appendix 1; p.443), but the species does not appear in any of her phylogenetic hypotheses. Concurrently, Frost et al. [23] resurrected the genus *Rhaebo* to accommodate species of the *Bufo guttatus* group of Blair [128]. They also transferred *Bufo ceratophrys* and *Bufo nasicus* to the genus *Rhinella*.

Finally, Frost [23], considering the evidence of Pramuk [121], transferred *Rhinella nasica* to *Rhaebo*, which remains the current taxonomy.

Fenolio et al. [119] recognized that the diagnosis of *Rhaebo ceratophrys* (as *Rhinella ceratophrys*) proposed by Hoogmoed [120] needed to be revised in the light of new collections. They performed a detailed morphological study and provided a new diagnosis for the species, recognizing it as having: (1) triangular projecting dermal flaps on the eyelids, (2) projecting dermal flaps at the corners of mouth, and (3) a larger adult size ([119]:10).

Ron et al. [95] studied the poorly known genus *Andinophryne* (now included in *Rhaebo*). They performed separate phylogenetic analyses for mitochondrial and

Table 1 Muscles origin and insertion in the larva of "*Rhaebo*" *nasicus*

Muscle	Origin	Insertion	Comments
Mandibular group, n. trigeminus (c.n. V) innervated			
Levator mandibulae longus superficialis	External posterior margin of subocular bar	Dorsomedial Meckel's cartilage	Via long tendon
Levator mandibulae longus profundus	External margin (curvature) of subocular bar	External margin of suprarostrale ala	Via a long tendon
Levator mandibulae longus internus	Ventral otic capsule and processus ascendens	Lateral Meckel's cartilage	Via a long tendon
Levator mandibulae externus superficialis	Inner muscular process (superior)	Adrostral tissue mass	
Levator mandibulae externus profundus	Inner muscular process (medial)	Distal suprarostrale ala	Share a tendon with LMLP
Levator mandibulae articularis	Inner muscular process (inferior)	Dorsal Meckel's cartilage	
Levator mandibulae lateralis	Articular process	Adrostral tissue mass	
Submentalis (intermandibularis anterior)	-	-	
Intermandibularis	Median aponeurosis	Ventromedial Meckel's cartilage	
Mandibulolabialis	Ventromedial Meckel's cartilage	Lower lip	
Mandibulolabialis superior	-	-	
Hyoid group, n. facialis (c.n. VII)			
Hyoangularis	Dorsal ceratohyal	Retroarticular process of Meckel's cartilage	
Quadratoangularis	Ventral palatoquadrate	Retroarticular process of Meckel's cartilage	
Suspensorioangularis	Ventral palatoquadrate	Retroarticular process of Meckel's cartilage	
Orbitohyoideus	Muscular process	Lateral edge of ceratohyal	
Suspensoriohyoideus	Posterior descending margin of muscular process and subocular bar	Lateral process of ceratohyal	
Interhyoideus	Median aponeurosis	Ventral ceratohyal	
Branchial group, n. Glossopharyngeus (c.n. IX) and vagus (c.n. X)			
Levator arcuum branchialium I	Lateral subocular bar	Ceratobranchial I	
Levator arcuum branchialium II	Lateral otic capsule	Ceratobranchial II	
Levator arcuum branchialium III	Lateral otic capsule	Ceratobranchial III	
Levator arcuum branchialium IV	Lateroventral otic capsule	Ceratobranchial IV	
Tympanopharyngeus	Lateroventral otic capsule	Ceratobranchial IV	
Constrictor branchialis I	-	-	
Constrictor branchialis II	Branchial process II	Terminal commissure I	
Constrictor branchialis III	Branchial process II	Terminal commissure II	
Constrictor branchialis IV	Ceratobranchial III	Terminal commissure II	I
Subarcualis rectus I	Posterior lateral base of ceratohyal	Branchial processes II and III, and ceratobranchial I	
Subarcualis rectus II-IV	Ceratobranchial IV	Ceratobranchial II	Lateral fibers invading the interbranchial septum IV
Subarcualis obliquus II	Urobranchial process	Ceratobranchials II	Single slip
Diaphragmatobranchialis	Peritoneum (diaphragm)	Distal Ceratobranchial III	
Spinal group, spinal nerve innervation			
Geniohyoideus	Hypobranchial plate	Infrastrale cartilage	At the level of CB III
Rectus abdominis	Peritoneum (diaphragm)	Pelvic girdle	Six open myomers
Rectus abdominis anterior	Peritoneum (diaphragm)	Ventral palatoquadrate	Very short fibers; via a long tendon
Rectus cervicis	Peritoneum (diaphragm)	Branchial process III	

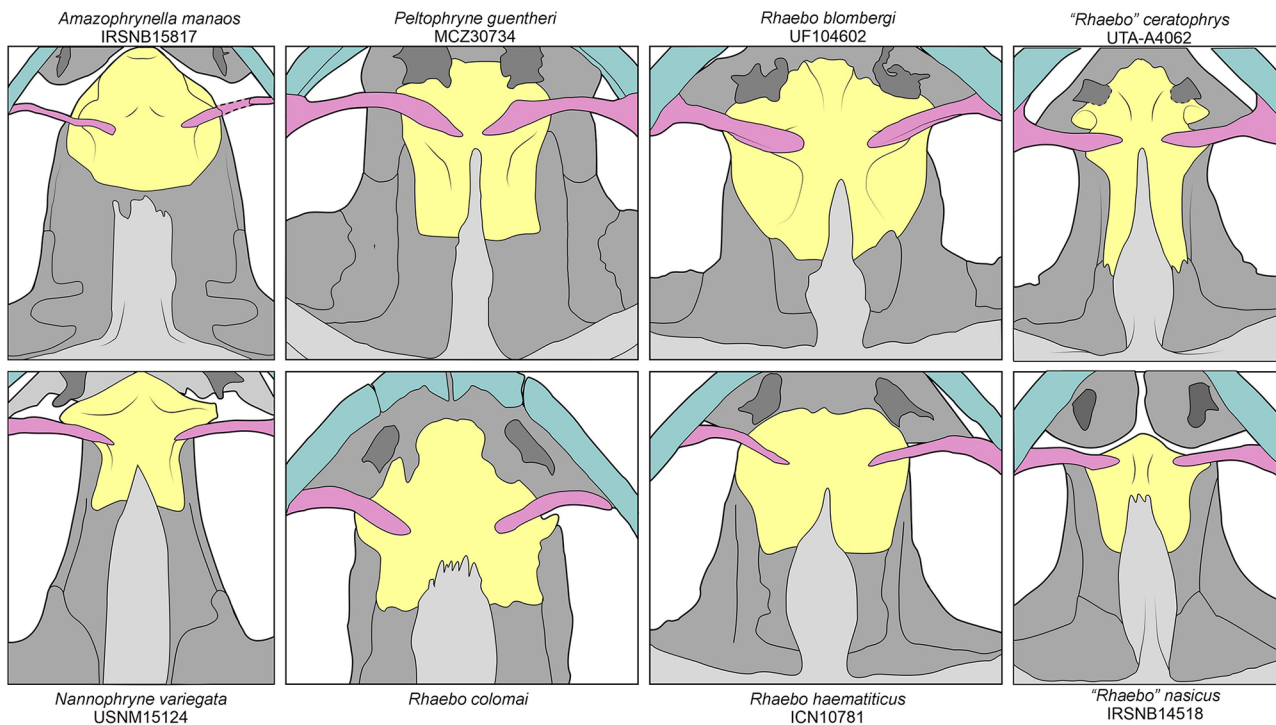


Fig. 11 Variation in the sphenethmoid morphology in *Amazophrynella*, *Nannophryne*, *Peltophryne*, and *Rhaebo* sensu lato (sl). Different cranial bones are colored as follows for reference: blue (maxilla and premaxilla), dark grey (vomeres), light grey (parasphenoid), pink (palatines), and yellow (sphenethmoid). Figures of *Peltophryne guentheri* and *Rhaebo colomai* were redrawn and slightly modified from [95] and [121]

nuclear data, placing *Andinophryne olallai* and *A. colomai* within *Rhaebo*—*Rhaebo nasicus* was sister to all other *Rhaebo*+*Andinophryne*. *Rhinella ceratophrys* was not included in that study. According to the authors, they preferred to synonymize *Andinophryne* with *Rhaebo* rather than erecting a new genus for *Rhaebo nasicus*, as their study did not include all *Rhaebo*. Other large-scale studies (e.g., [129–130]) have also recovered *Rhaebo nasicus* as sister to all other *Rhaebo* (Fig. 12).

Pereyra et al. [96] studied the evolution and systematics of *Rhinella* with a large and dense taxon sampling (including an extensive outgroup sampling). They included representatives of *Rhinella ceratophrys* in a phylogenetic analysis for the first time. In their total evidence analysis under Maximum Parsimony ([96]: Fig. 10), they recovered *Rhaebo nasicus* as sister to *Rhinella ceratophrys* and the rest of *Rhaebo* as sister to *Rhaebo nasicus* and “*Rhinella*” *ceratophrys*+other bufonids, rendering both *Rhinella* and *Rhaebo* non-monophyletic. The authors transferred *R. ceratophrys* to *Rhaebo*, despite the paraphyly of *Rhaebo*, arguing that their analysis was not designed to rigorously test the monophyly of *Rhaebo*.

Recently, Portik et al. [97] published a large study on the phylogeny of anurans. They included seven of the 14 valid species assigned to *Rhaebo*. In their topology, *Rhaebo nasicus* and *Rhaebo ceratophrys* are sister taxa and together form the sister group to all other *Rhaebo*.

In summary, neither *Rhaebo nasicus* or *R. ceratophrys* have ever been recovered as nested within other *Rhaebo* species in any phylogenetic hypothesis (Fig. 12) and the most inclusive analysis of Bufonidae strongly supports the clade formed by *Rhaebo nasicus* and *R. ceratophrys* as the sister clade to all other *Rhaebo*. The larval morphology of other *Rhaebo* species is a generalized, benthic type (e.g., [131–132]), while the larval morphology of *R. nasicus* (and likely *R. ceratophrys*) is a specialized torrential form (see above). Therefore, combining larval and adult morphological synapomorphies for the clade of *R. nasicus* and *R. ceratophrys* (e.g., [96, 119, 120]; this study), along with phylogenetic evidence supporting their monophyly ([96, 97]; this study), we propose that this clade should be recognized as new genus, which is named hereafter.

Taxonomic account

Adhaerobufo gen. nov.

ZooBank registration urn: lsid: zoobank.org: act: C757A1FA-A343-4134-8371-6A42797F162A

Type species *Bufo nasicus* (Werner, 1903 [125]) comb. nov.

Immediately more inclusive taxon Bufonidae Gray, 1825 [134].

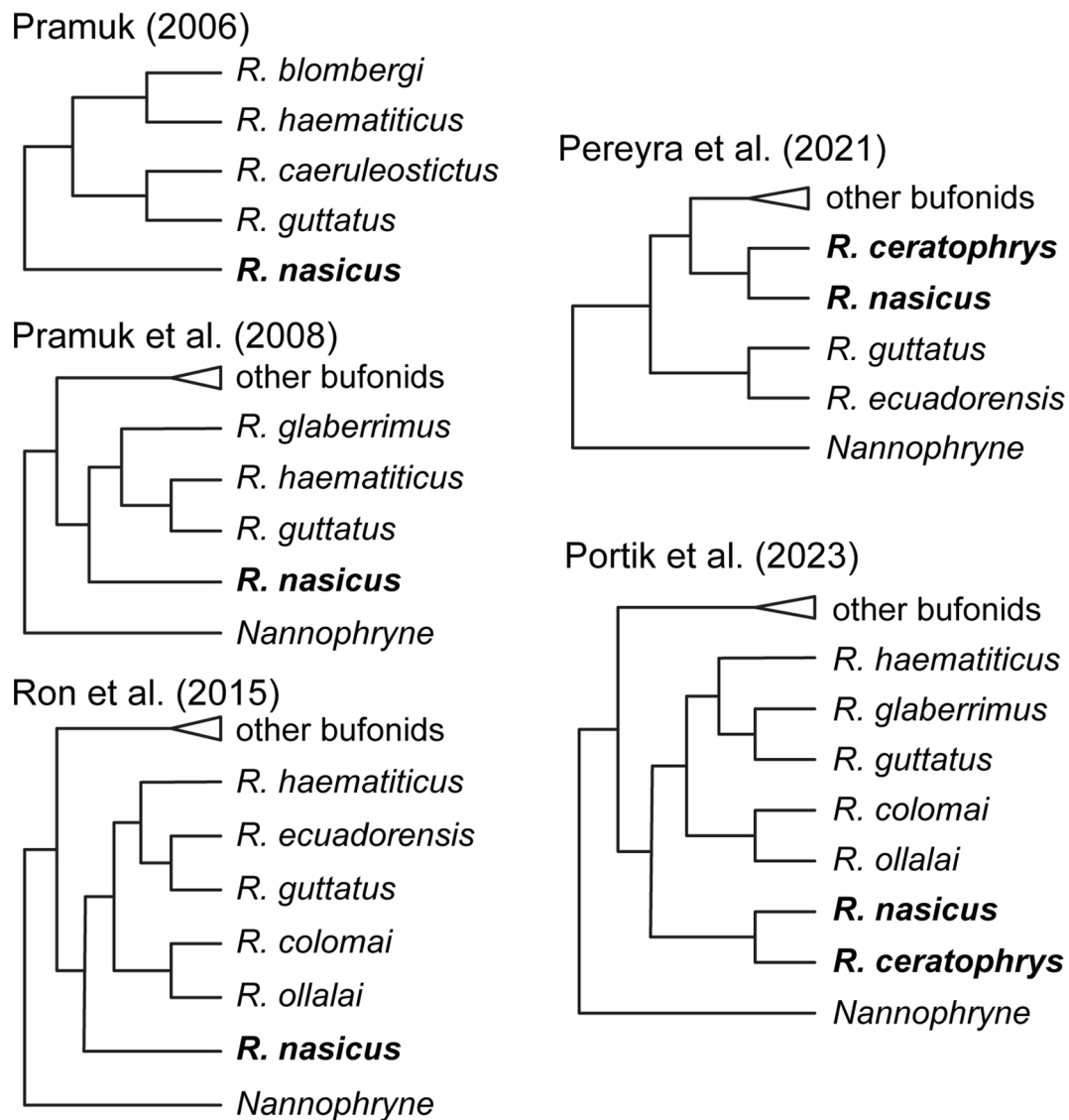


Fig. 12 Summarized relationships of “*Rhaebo*” *nasicus* (and *R. ceratophrys* when included) according to the several published phylogenetic hypotheses for Bufonidae: Pramuk ([121]: Fig. 1; morphological data alone, MP tree); Pramuk et al. ([133]: Fig. 1; molecular data alone, Bayesian analysis tree); Ron et al. ([95]: Fig. 1; molecular data alone, ML tree); Pereyra et al. ([96]: Fig. 10; phenotypic+ molecular data, MP tree), and Portik et al. ([97]: Fig. 57; molecular data alone, ML tree)

Content *Adhaerobufo ceratophrys* (Boulenger, 1882 [122]) comb. nov, and *Adhaerobufo nasicus* (Werner, 1903 [125]) comb. nov.

Etymology *Adhaerobufo* gen. nov. (gender masculine) is derived from the Latin *adhaerens*, meaning adherent and the Latin *būfo*, meaning toad. The name refers to the unique suctorial morphology of their tadpoles.

Definition and diagnosis: *Adhaerobufo* gen. nov. can be differentiated from all other Bufonidae by the combination of the following characters: (1) tadpole with enlarged, suctorial, oral disc; (2) tadpole oral disc with a complete

row of marginal papillae; (3) tadpole oral disc with multiple rows of submarginal papillae on the lower lip and by a single row of marginal papillae on the upper lip; (4) tadpole oral disc with an uninterrupted second anterior row of keratodonts; (5) presence of the m. interhyoideus posterior at larval stage; (6) presence of the m. rectus abdominis anterior at larval stage; (7) presence of narial vacuities in the buccopharyngeal cavity at larval stage; (8) projecting, enlarged eyelid in adults; (9) presence of an infraocular cream spot in adults, (10) sphenethmoid relatively narrow, overlapping only the medial ends of the palatines; and (11) posterior process of the prootic prominent and notched.

Comment The genetic diversity observed in *Adhaerobufo* **gen. nov.** strongly suggests the occurrence of at least one additional species within the genus (see Appendix MS3). Given the imprecise type locality of *A. nasicus* and the high genetic divergence observed between the sequences of the tadpole and adult specimens from several different localities, there is likely a hidden diversity in the genus, with more species to be described.

Further comparisons with other genera

Larval characters

Adhaerobufo **gen. nov.** presents several of the bufonid larval synapomorphies, such as the absence of the m. diaphragmatopraecordialis, the lateral fibers of m. subarcualis rectus II-IV invading branchial septum IV, the larval lungs being rudimentary or absent, and presence of single pairs of infralabial papillae. Nevertheless, it lacks other bufonid synapomorphies, such as the oral disc with a wide ventral gap in marginal papillae and the absence of the m. interhyoideus posterior.

The complete row of marginal papillae differentiates *Adhaerobufo* **gen. nov.** from all other bufonids, including other members of *Rhaebo*. The enlarged, suctorial disc differentiates *Adhaerobufo* **gen. nov.** from all other bufonids except *Ansonia*, *Blaira*, *Phrynoidis*, and *Werneria*. The lack of a belly sucker differentiates it from *Adenomus*, *Atelopus*, *Bufo* (part; *Bufo aspinus*), *Rhinella* (part; *Rhinella veraguensis* group), and *Sabahphrynus*. The uninterrupted second anterior row of keratodonts differentiates *Adhaerobufo* **gen. nov.** from most genera, except *Amazophrynella*, *Phrynoidis*, and *Werneria* (although some few species within some genera, such as, *Adenomus*, *Ansonia*, *Atelopus*, *Bufo*, *Bufotes*, *Capensibufo*, *Ingerophrynus*, *Melanophryniscus*, *Rhinella*, and *Sclerophrys*, have been reported lacking the interruption). The multiple rows of submarginal papillae in the lower lip and a single row of marginal papillae in the upper lip differentiate *Adhaerobufo* **gen. nov.** from all genera but *Werneria*. The presence of the m. interhyoideus posterior differentiates it from all other bufonids except *Amazophrynella*. Finally, the presence of narial vacuities in the buccopharyngeal cavity differentiates *Adhaerobufo* **gen. nov.** from all other bufonids except *Ansonia*, *Atelopus*, *Incilius* (part; *Incilius coniferus*), *Schismaderma*, and *Werneria*.

Several *Rhaebo* species have their tadpoles described, including *R. glaberrimus*, *R. guttatus*, *R. haematiticus*, and *R. caeruleostictus* (e.g., [131, 132, 135]). None of these species has a suctorial form, and most typify the benthic, lentic type common across bufonids. Several other members of the genus have no published data on tadpole morphology, and to our knowledge no collections have been made. Previous attempts to collect the tadpole of *Rhaebo olallai* have been unsuccessful, and

while recently metamorphosed froglets were found alongside a fast-flowing mountain stream in the Ecuadorian Andes, no tadpoles were found within the stream ([136], Trageser S., pers comm).

Finally, we would like to stress that a phenotypically similar tadpole from Amazonia, which shares all external morphology characters with *A. nasicus*, including the color pattern, the enlarged oral disc, and the complete row of marginal papillae, is awaiting formal description (T. Grant and T. Pezzuti, pers comm). Individuals of that species in late Gosner developmental stage [111] present a dorsal color pattern very similar to that of adults of *A. ceratophrys* (thus contra juveniles of *Rhaebo* [95]). Likewise, juveniles of *A. nasicus* have the same color pattern as adults, both in life and in preservative.

Adult characters

As noted by Hoogmoed [120], *Adhaerobufo nasicus* and *A. ceratophrys* share a projecting flap above the eyelid. This character is especially pronounced in *A. ceratophrys*, where it is enlarged to form a spiny projection above the eye. The lateral surfaces of head and body (including the ventral portion of the parotoid macroglands) in *Adhaerobufo* **gen. nov.** are dark, similar to some species of *Rhaebo* (e.g., *R. blombergi*, *R. guttatus*, *R. haematiticus*). Nevertheless, both species have a well-defined infraocular cream spot. The combination of dark pattern contrasting with an infraocular cream spot is a putative synapomorphy of *Adhaerobufo* **gen. nov.**, as it does not occur in other related genera of Bufonidae. *Adhaerobufo* **gen. nov.** shares several characters previously associated with *Rhaebo*, including an elongate transverse process of vertebra VI, well-developed omosternum, and large and notched posterior processes of the prootic ([95]: Fig. 6 for *R. blombergi* and *R. colomai*, the authors pers. obs.). *Adhaerobufo* **gen. nov.** differs from *Rhaebo* in having a distinctly narrow sphenethmoid.

Distribution (Fig. 13)

Northwestern Guyana and eastern Venezuela (*Adhaerobufo nasicus*) and upper Amazon Basin in western Brazil, southeastern Colombia, eastern Ecuador, northeastern Peru, and southern Venezuela (*A. ceratophrys*).

Natural history

Tadpoles of *Adhaerobufo nasicus* were scraped by aquarium-mesh dip-net from the sides of large, submerged boulders of Roraima Supergroup sandstones in the bed of Kamana Creek, upstream within 100 m of Kamana Waterfall (Fig. 14A), draining Mt. Kopinang, one of the peaks of the Wokomung Massif, Potaro-Siparuni District, Guyana. Tadpoles were observed clinging by their mouthparts to the vertical sides of big boulders on 7 December 2006 (DBM-3372); 18 July 2007 (observed

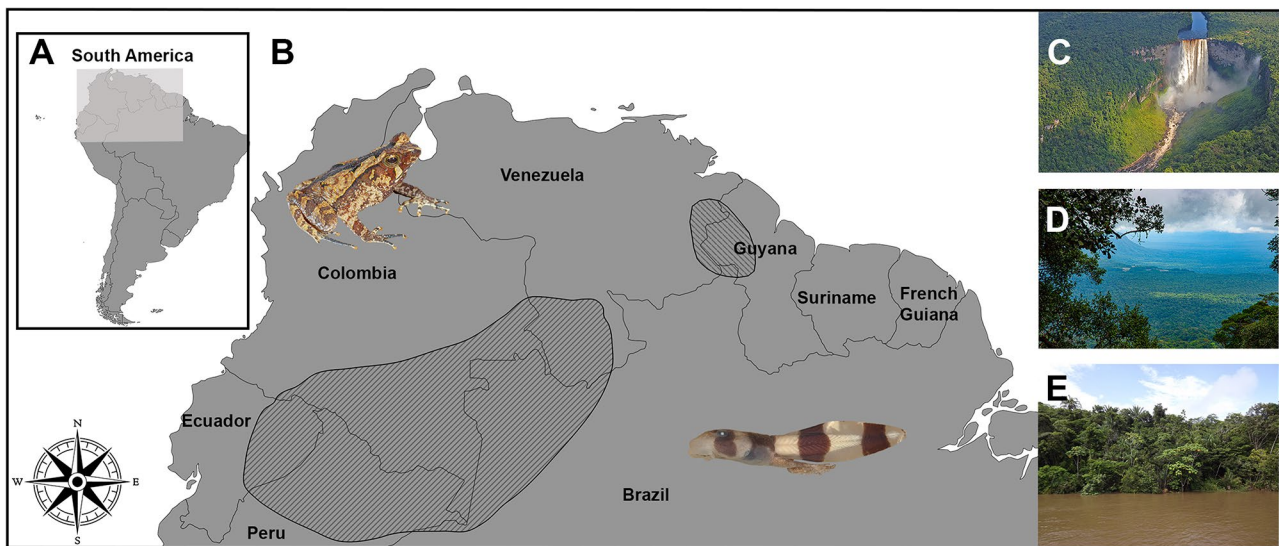


Fig. 13 Geographical distribution of *Adhaerobufo* gen. nov. in northwestern Guyana, eastern Venezuela and upper Amazon Basin. Inset map of South America, highlighting the geographical area occupied by the genus (A). Known distribution of *A. ceratophrys* and *A. nasicus* (B). Examples of macrohabitats in which the new genus is present; Kaieteur Falls in Guyana (C), uplands and highlands of western Guyana (D), and lowlands, Amazon Forest, Ica River, Brazil (E). Shape files of the geographical distribution were downloaded from the IUCN website. Adult and tadpole are from *A. nasicus*. Photos by: Philippe Kok (C and D) and Pedro H. Dias (E)

when water was shallow on 18 July but not collected on 19 July due to torrential flow overnight); and 25 June 2012 (CPI10704). Figure 12B is a view of an unnamed stream on the slopes of Maringma-tepui on 22 November 2007 where *Adhaerobufo* tadpoles were also observed (same ecological data as above). Figure 14C–D are of an amplexing pair of *A. nasicus* in situ (Wokomung Massif) when first discovered on 20 July 2012 (14 C), and shortly thereafter when placed on a leaf for photography (14D). Amplexus is inguinal, and couples have been observed in shallow waters, on the side of rivers. Tadpoles and adults were observed in similar microhabitats at the base and on the slopes of Maringma-tepui in western Guyana in November 2007 (e.g., Fig. 14B), and in the La Escalera region of Venezuela in November 2010. Adult individuals were collected/observed all year long in Kaieteur National Park (west-central Guyana), although tadpoles were not found at that location. In Kaieteur National Park adults were often found relatively far away from any fast-flowing streams suggesting either periodical migration to suitable breeding sites, or plasticity in egg deposition site. Since we never collected any *A. nasicus* tadpole in non-flowing waterbodies, we favor the first hypothesis.

Discussion

Larval morphology, systematics, and taxonomy

The impact of larval morphology on the systematics of bufonids has been widely discussed recently [33, 63]. Larval synapomorphies of Bufonidae are: (1) oral disc with wide ventral gap in marginal papillae; (2) anterolateral process of crista parotica absent; (3) m.

diaphragmatopraecordialis absent; (4) lateral fibers of m. subarcualis rectus II–IV invading branchial septum IV; (5) larval lungs rudimentary or absent; (6) the m. interhyoideus posterior absent; and (7) a single pair of infralabial papillae [21, 33, 47, 63]. Additionally, several synapomorphies have been reported for less inclusive clades (e.g., [33, 60, 63, 137, 138]).

Adhaerobufo nasicus shares several of these synapomorphies, but reverted some states; for instance, it is characterized by the complete row of marginal papillae and by presenting the m. interhyoideus superior. Additionally, other autapomorphic traits are present in the larvae of *Adhaerobufo* gen. nov., such as (1) the enlarged, suctorial, oral disc; (2) multiple rows of submarginal papillae in the lower lip and by a single row of marginal papillae in the upper lip; and (3) the presence of narial vacuities in the buccopharyngeal cavity. The combination of traits supports *Adhaerobufo* gen. nov. in Bufonidae but also distinguishes it from all other bufonids.

Adhaerobufo gen. nov. has been consistently recovered as either sister taxon of *Rhaebo* (e.g., [96, 97, 121]; this work, Fig. 2) or closely allied to this genus ([96]; this work Fig. Figure 1) and the morphology of their larvae is unique—especially in comparison with “typical” *Rhaebo* larvae (Fig. 15)—including several apomorphic transformations, supporting our proposition of a new genus. Furthermore, additional characters from adult morphology and osteology also underscore the distinctiveness of this taxon. The genus *Rhaebo* has relatively few potential synapomorphies, and the widened shape of the sphenethmoid has been used previously as an important

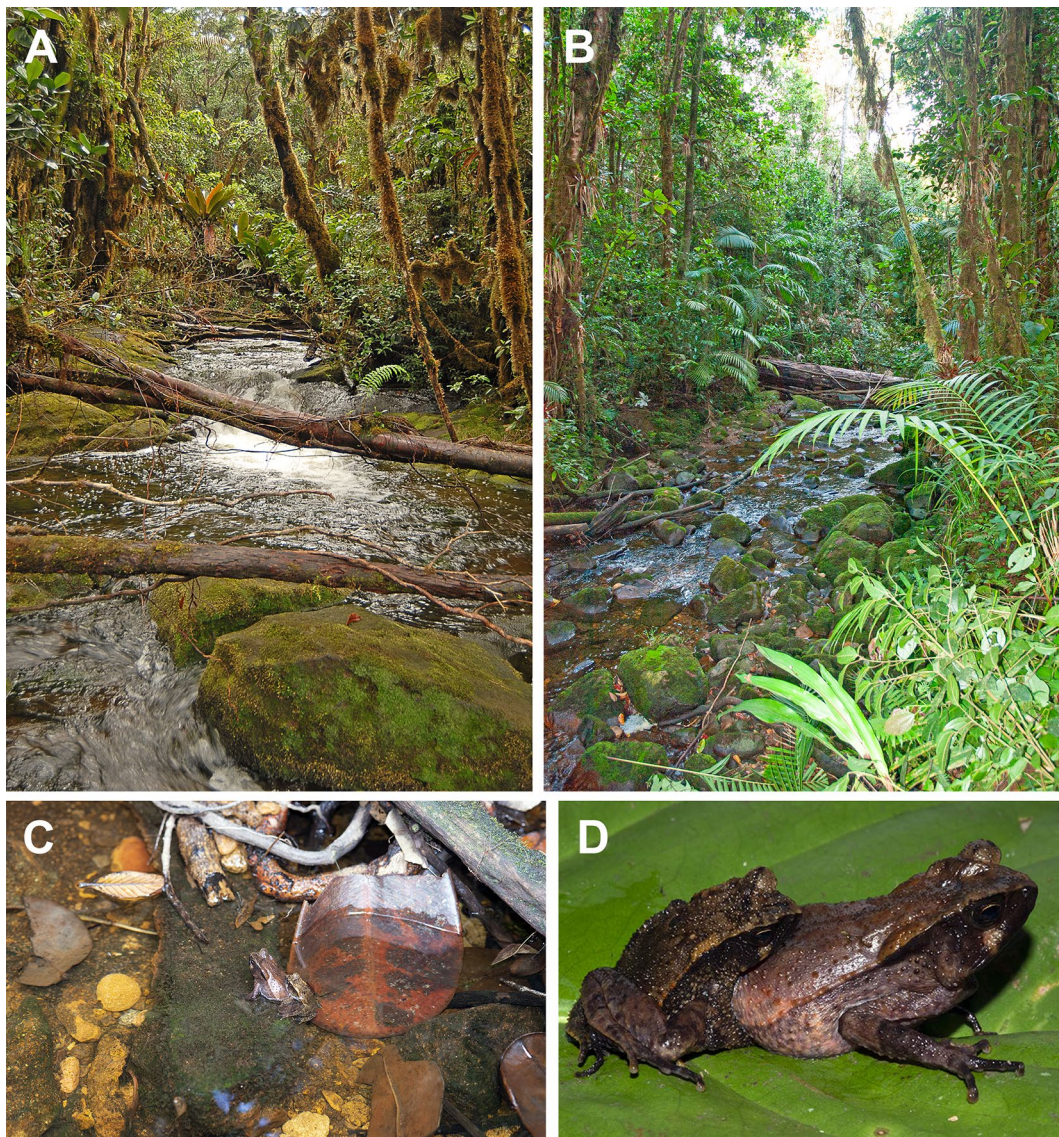


Fig. 14 Kamana Creek, upstream within 100 m of Kamana Waterfall, draining Mt. Kopinang low waters where tadpoles of *Adhaerobufo* were collected (A) and an unnamed stream on the slopes of Maringma-tepui where tadpoles were also observed (B). Amplexing couple of *A. nasicus* (C and D). Photos by D. Bruce Means (A, C, D) and Philippe J. R. Kok (B)

generic trait. We find that *Adhaerobufo* **gen. nov.** lacks this character, therefore, the inclusion of *A. nasicus* and *A. ceratophrys* in *Rhaebo* would potentially destabilize its taxonomy. Additionally, by recognizing *Adhaerobufo* **gen. nov.** as a new genus, *Andinophryne* can be revalidated without affecting the monophyly of *Rhaebo*. We refrained from making this change, as we have not personally examined specimens of *R. olallai* or *R. colomai*. Furthermore, Ron et al. [95] suggested some phenotypic characters, including a widened sphenethmoid, to support *Andinophryne* as part of *Rhaebo*.

Ron et al. [95] also mentioned that the coloration pattern of juveniles, described as “dorsal coloration consisting of a dark background with contrasting thin clear

stripes or dots”, could be a synapomorphy of *Rhaebo*. The fact that (1) tadpoles closely related to *A. ceratophrys* (see above) in late developmental stage already present the adult dorsal color pattern; and (2) that juveniles of *A. nasicus* have the same color pattern as the adults suggests that the synapomorphy proposed by Ron et al. [95] supports the monophyly of *Rhaebo*, including *Andinophryne*. Nevertheless, just as in *Rhaebo* sl, *Peltophryne* juveniles change their color pattern (e.g., [139, 140], which could affect the optimization of that character. Thus, we recommend caution when considering this potential synapomorphy. The present results reinforce the potential of larval morphology in the fields of systematics, taxonomy, and evolution. Tadpoles are highly variable regarding



Fig. 15 Phenotypic differences between *Adhaerobufo nasicus* (CPI10704) (A) and *Rhaebo* larvae; *R. caeruleostictus* (KU112307) (B) and *R. haematiticus* (KU68327) (C). Note the striking differences in body shape, mouthparts, and coloration. Scale bars = 1.0 mm. Photos by: Pedro H. Dias (A) and Jackson Phillips (B and C)

their morphology (e.g., [25, 27, 28, 35, 43, 138, 141, 142]), ecology and behavior (e.g., [143, 144]), among others. Such variation makes tadpoles a powerful source of evidence to test hypotheses of evolutionary relationships among frogs. Recently, several studies have approached larval morphology in a phylogenetic context (e.g., [35, 45]), resulting in the identification of novel synapomorphies and strengthening the support of clades.

It is also evident that the exploration of larval morphology in previously unstudied groups has widened our perception of larval diversity. In the past 20 years, astonishing novel phenotypes have been reported (e.g., [27, 28, 141]), but many of these new characters have never been included in any phylogenetic analysis. We strongly advocate for the usage of larval morphology in further studies about the evolution and diversification of anurans.

Finally, we believe that the taxonomy of anurans (and of other organisms with complex life cycles) could greatly benefit from the usage of non-adult semaphoronts. Historically, anuran taxonomists have concentrated their efforts in metamorphosed adult (mainly males), ignoring

larval individuals. When such dogma is broken, taxonomists can better delimit, recognize, and describe species, and other supraspecific clades. For example, Grosjean et al. [24] were able to describe *Clinotarsus penelope* (Ranidae), referring a tadpole as the holotype. Our study follows the same path, and larval characters were pivotal for the proposition of *Adhaerobufo* gen. nov. – named after larval characteristics.

The evolution of suctoriality in bufonid tadpoles

Recently, Dias and Anganoy-Criollo [33] discussed the convergent evolution of suctorial and gastromyzophorous ecomorphologies across anurans. They stressed that the presence of enlarged oral disc and/or of a belly sucker were different strategies shaped by natural selection in tadpoles occupying fast-flowing waters. These strategies have evolved independently multiple times across 13 families of anurans. These authors, however, also discussed the differences among these larvae, suggesting that the real diversity of suctorial forms is unknown.

Suctorial and gastromyzophorous larvae evolved independently at least 10 times in Bufonidae (Fig. 16). Gastromyzophorous tadpoles have been reported in all known *Atelopus* larvae, in three species of the *Rhinella veraguensis* group (*R. chrysochora*, *R. quechua*, and *R. veraguensis*), in *Sabahphrynus maculatus*, in *Adenomus kandianus*, and in *Bufo aspinius* [33, 60, 145–147], whereas suctorial tadpoles have evolved in *Adhaerobufo gen. nov.*, *Ansonia*, *Blaira*, *Phrynoidis*, *Bufo pageoti*, *Bufo torrenticola*, *Bufo tuberospinus*, and *Werneria* ([66, 148–151]; the present study).

As stressed by Dias and Anganoy-Criollo [33], suctorial larvae of bufonids share many traits, but also differ widely. Suctorial larvae share a series of convergent traits, such as the presence of a developed element in

the prenarial arena and of narial vacuities [33], a widening of the palatoquadrate, enlarged and short cornua trabeculae, robust lower jaw, upper jaw with fused elements and with a well-developed processus posterior dorsalis, adrostral elements often present, reduction of elements of the branchial basket, modifications in the insertion of the abdominal muscles, presence of a rectus abdominis superior, suspensorio-angularis with a sub- or postorbital origin, and well developed axial muscles ([21, 47, 60, 152]; PHD, the authors, pers. obs.). Each independent instance of bufonid suctoriality is also unique. The most obvious difference among many is the presence of a belly sucker in gastromyzophorous species, as opposed to an enlarged oral disc, but there are other variable states. For instance, jaw sheaths are interrupted in *Ansonia*,

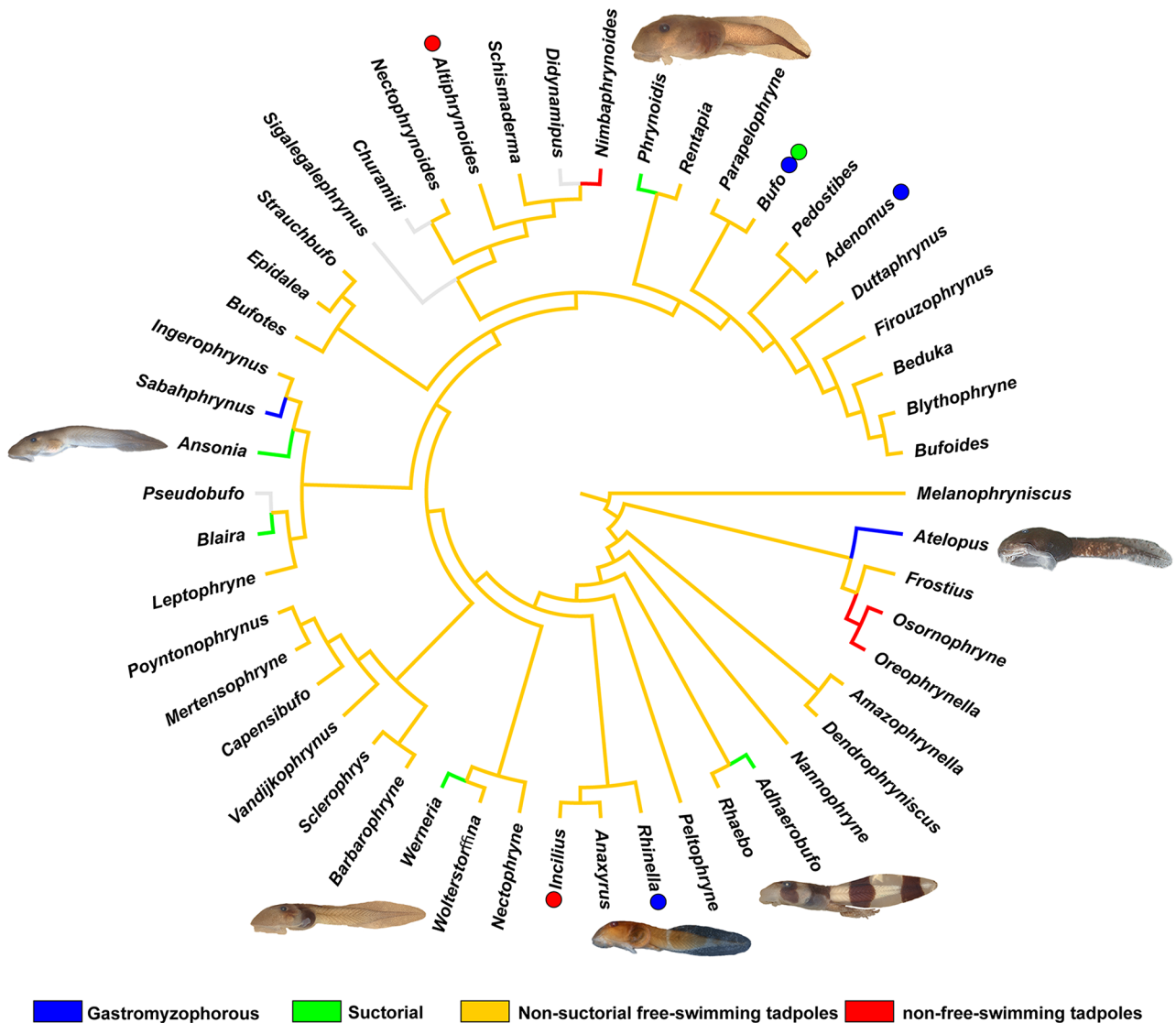


Fig. 16 Gastromyzophorous and suctorial larvae evolved independently at least 10 times within bufonids, revealed by the phylogenetic hypothesis of Portik et al. [95] showing the genera in which these tadpoles have evolved. The dots next to the genera indicate derived conditions within them. Photos by: Pedro H. Dias and Jackson Phillips

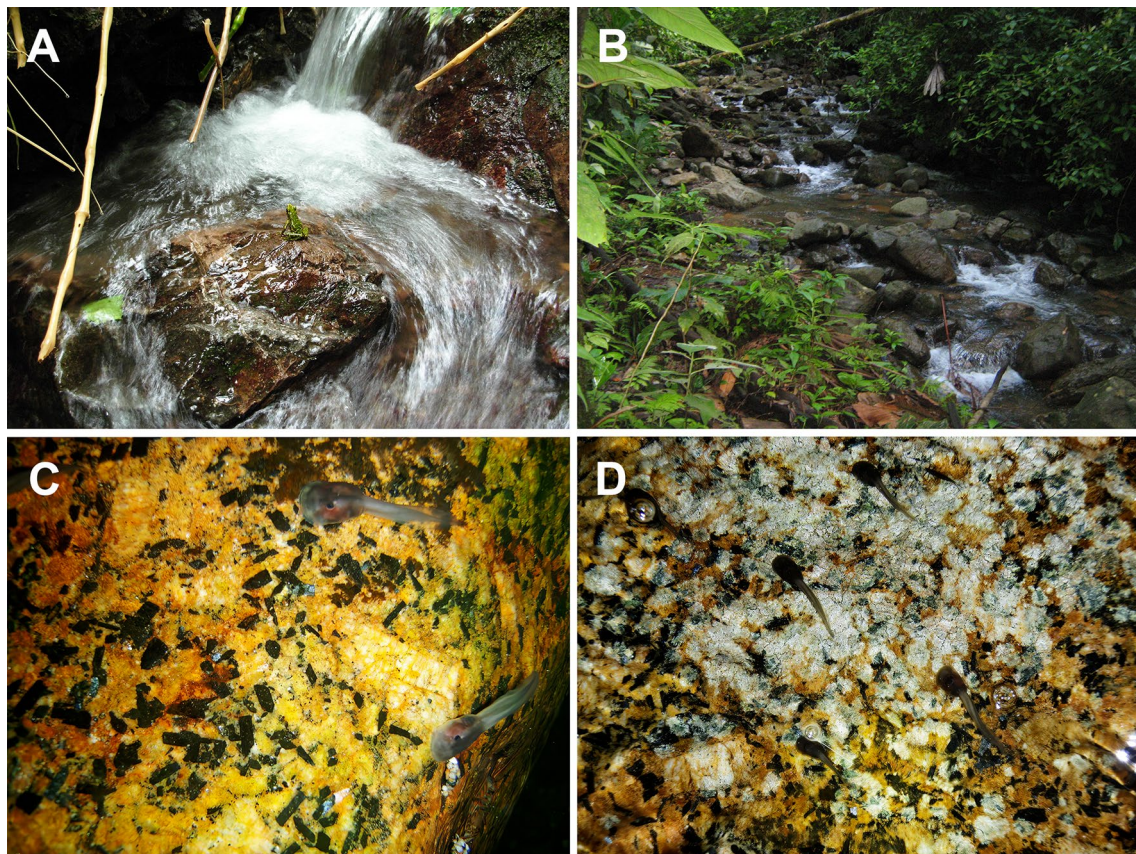


Fig. 17 Torrential environments that were colonized by suctorial/gastromyzophorous larvae of bufonids. Adult of *Atelopus* sp. in Tacarcuna, Colombia (A); fast flowing waters occupied by *Atelopus elegans* at Isla Gorgona, Colombia (B); larvae of *Ansonia guibei* attached to rocks of fast flowing streams in Borneo (C and D). Photos by Marco A. Rada (A), David Velázquez (B), and Alexander Haas (C and D)

but continuous in other taxa. Other variable characters are the presence and distribution of submarginal papillae, tail tip morphology, and body color pattern. Despite the great potential of this system in the study of novelty and ecomorphological evolution, the significance of such variation remains largely unexplored.

Adhaerobufo gen. nov. represents an interesting case, given that the adult form is rather unspectacular, being confused with many unrelated bufonid sub-clades over time. It is remarkable that the adult form appears to be so unaffected by radical evolutionary changes to the larva. We interpret this as further evidence of the decoupling power of metamorphosis, whereby evolutionary changes in the larval form can operate semi-independently of the adult phenotype, despite sharing a genome and being part of the same developmental sequence [153–154]. From a macroevolutionary perspective, it is interesting to note that the evolution of suctoriality may be particularly common in bufonids. Vera Candiotti et al. [57] demonstrated that suctorial forms are the exclusive larval form of four anuran families, (Ascaphidae, Conrauidae, Heleophrynidae, and Nasikabatrachidae), and that while suctoriality has evolved in several other families,

it is a relatively rare phenomenon in anurans (number of suctorial species/number of species). Future studies that identify the features that make suctoriality a more common evolutionary outcome in some lineages (including bufonids) than others could provide insight into not only adaptive ecomorphological evolution, but also non-adaptive factors that limit such evolutionary changes.

Conclusion

We describe the tadpole of “*Rhaebo*” *nasicus* and present evidence supporting the erection of a new genus, *Adhaerobufo* gen. nov., to recognize the evolutionary distinctiveness of this group of South American toads. The tadpole of *Adhaerobufo nasicus* is a brightly colored, suctorial form adapted to living in fast-flowing streams. The oral morphology of that tadpole is unique among bufonids, with a complete row of marginal papillae that differentiates it from all other tadpoles known from the family Bufonidae. Suctorial larvae have evolved independently at least 10 times in bufonids; in each case, a combination of convergent and unique traits can be observed. Our findings echo the importance of tadpoles in systematic and taxonomic studies.

Abbreviations

ALPH	Antelateral process hyalis
AP	Articular process
APH	Anterior process hyalis
AT	Adrostral tissue
BFA	Buccal floor arena
BFAP	Buccal floor arena papillae
BRAP	Buccal roof arena papillae
CB	Constrictor branchialis
CH	Ceratohyal
DV	Dorsal velum
HA	Hyoangularis
HP	Hypobranchial plate
HQP	Hyoquadrate process
IH	Interhyoideus
IHP	Interhyoideus posterior
ILP	Infralabial papillae
IM	Intermandibularis
IN	Internal nares
IR	Infrarostral cartilage
JAF	Jackknife absolute frequencies
JF	Jugular foramen
JGC	Parsimony jackknife frequency differences
LMA	Levator mandibulae articularis
LMEP	Levator mandibulae externus profundus
LMES	Levator mandibulae externus superficialis
LMI	Levator mandibulae internus
LMLS	Levator mandibulae longus superficialis
LP	Lateral process
LR	Lateral ridge
LTRF	Labial tooth row formula
MC	Meckel's cartilage
μCT	High-Resolution micro-computed tomography
ML	Maximum likelihood
MP (in larval cranium)	Maximum parsimony
MP (in phylogenetics)	Muscular process
MR	Median ridge
NV	Narial vacuities
OH	Orbitohyoideus
OC	Otic capsule
PCM	Proximal commissure
PNP	Postnarial arena papillae
PP	Posterior process
PU	Process urobranchialis
QA	Quadrato-angularis
QOC	Quadro-Orbital commissure
RA	Rectus abdominis
RAA	Rectus abdominis anterior
RC	Rectus cervicis
SA	Suprarrostral ala
SAR I	Subarcualis rectus I
SAR II-IV	Subarcualis rectus II-IV
SB	Subocular bar
SC	Suprarrostral copora
SH	Suspensoriohyoideus
SO	Subarcualis obliquus
SP	Spicule
TA	Tongue anlage
TH	Trabecular horns
TP	Triangular projection
TS	Tectum synoticum
TTM	Taenia tecti medialis
TTT	Taenia tecti transversalis
UFBoot	Ultrafast Bootstrap Approximation
UJ	Upper Jaw Sheath
VV	Ventral Velum

Supplementary Information

The online version contains supplementary material available at <https://doi.org/10.1186/s40851-024-00241-0>.

Supplementary Material 1: Appendix MS1 take ESM 1

Supplementary Material 2: Appendix MS2 take ESM 2

Supplementary Material 3: Appendix MS3 take ESM 3

Supplementary Material 4: Appendix MS4 take ESM 4

Supplementary Material 5: Figure MS5 take ESM 5

Supplementary Material 6: Figure MS6 take ESM 6

Acknowledgements

Pedro H. Dias thanks the Marie Skłodowska-Curie Actions (MSCA-IF-2020, MEGAN/101030742). We thank the Smithsonian Institution and curatorial staff for providing specimens for examination and scanning. The work of Jackson R. Phillips was supported by start-up funds awarded to Molly C. Womack by Utah State University. Martín O. Pereyra acknowledges the support from Agencia Nacional de Promoción Científica y Tecnológica (ANPCyT PICTs 2019–346, 2019–2519, 2019–2557) and Consejo Nacional de Investigaciones Científicas y Técnicas (CONICET PIP 11220200102800CO). Fieldwork of D. Bruce Means was supported by a National Geographic Society Expeditions Council Grant and Guyana EPA permission to conduct Biodiversity Research (Reference Numbers 1007003 BR 0098; 011206 BR 065; 120707 BR 075; 061212c BR 020) and to export specimens for scientific research (Reference Numbers 030310 SP 001; 151206 SP 030; 230707 SP 008; 072412 SP 054). The work of Philippe J. R. Kok was supported by a Marie Skłodowska-Curie Actions grant (MSCA-IF-2020, HOSTILE/101022238). We thank Marco Rada and David Velázquez for kindly providing photos of the environment occupied by *Atelopus* species. Olivier Pauwels kindly provided access to the individual housed at the Royal Belgian Institute of Natural Sciences. Agustín Elias-Costa contributed to the improvement of Fig. 11. We also thank Kevin de Queiroz, Esther Langan, and the Smithsonian Institution, Eric Smith, Greg Pandalis, and the University of Texas Arlington ARDRC, as well as Rafe Brown, Ana Motta, and the Kansas University Biodiversity Institute and Natural History Museum for providing specimens and permission for CT scanning. David Blackburn, contributors, and the staff of MorphoSource (Duke Library Digital Repository) made μCT images of relevant species available. Daniel Paluh shared μCT images of *Amazophrynella*. Finally, we thank three anonymous reviewers for comments that improved the quality and clarity of our manuscript.

Author contributions

Pedro H. Dias and Jackson R. Phillips conceived and designed the study. Philippe J. R. Kok and D. Bruce Means acquired samples. Pedro H. Dias, Philippe J. R. Kok and Martín O. Pereyra acquired funding. Pedro H. Dias, Jackson R. Phillips, Martín O. Pereyra and Philippe J. R. Kok performed the analyses and analyzed the data. Pedro H. Dias and Jackson R. Phillips wrote the original draft with inputs by all authors. Pedro H. Dias, Jackson R. Phillips, Martín O. Pereyra, and Philippe J. R. Kok prepared/contributed to all figures.

Funding

This work was supported by two Marie Skłodowska-Curie Actions (MSCA) grants (MEGAN/101030742 to Pedro H. Dias and HOSTILE/101022238 to Philippe J. R. Kok). Martín O. Pereyra is supported by the Agencia Nacional de Promoción Científica y Tecnológica (ANPCyT PICTs 2019–346, 2019–2519, 2019–2557) and the Consejo Nacional de Investigaciones Científicas y Técnicas (CONICET PIP 11220200102800CO). Fieldwork of D. Bruce Means was supported by a National Geographic Society Expeditions Council grant.

Data availability

Further information and requests for additional resources should be directed to and will be fulfilled by the corresponding authors. This article has been registered in ZooBank with the life science identifier urn: lsid: zoobank.org: pub: 95161DF6-0C46-4CC1-9BD1-045545B57C57.

Declarations**Ethical approval**

Not applicable.

Consent for publication

Not applicable.

Competing interests

Not applicable.

Received: 8 April 2024 / Accepted: 13 August 2024

Published online: 30 September 2024

References

1. Lataste MF. Étude sur le discoglosse. Actes Soc linn Bordeaux. 1879;33:275–341.
2. Pizarro JJ. Nota descriptiva de um pequeno animal extremamente curioso e Denominado Batrachychthys. Arch Mus Nac. 1876;1:31–5.
3. Noble GK. An outline of the relation of ontogeny to phylogeny within the Amphibia I. Am Mus Novit. 1925;165:1–17.
4. Noble GK. An outline of the relation of ontogeny to phylogeny within the Amphibia II. Am Mus Novit. 1925;166:1–10.
5. Noble GK. The integumentary, pulmonary, and cardiac modifications correlated with increased cutaneous respiration in the amphibia: a solution of the hairy frog problem. J Morphol. 1925;40:341–416.
6. Noble GK. The importance of larval characters in the classification of South African Salientia. Am Mus Novit. 1926;237:1–10.
7. Noble GK. The value of life history data in the study of the evolution of the Amphibia. Ann NY Acad Sci. 1927;30:31–129.
8. Noble GK. The adaptive modifications of the arboreal tadpoles of *Hoplophryne* and the torrent tadpoles of Staurois. Bull Am Mus Nat Hist. 1929;58:291–330.
9. Orton GL. The systematics of vertebrate larvae. Syst Zool. 1953;2:63.
10. Orton GL. The bearing of larval evolution on some problems in frog classification. Syst Zool. 1957;6:79–86.
11. Griffiths I. The phylogeny of the salientia. Biol Rev Camb Philos Soc. 1963;38:241–92.
12. Griffiths I, de Carvalho AL. On the validity of employing larval characters as major phyletic indices in Amphibia, Salientia. Rev Bras Biol. 1965;25:113–21.
13. Dias PHS, Carvalho-e-Silva AMPT, Carvalho-e-Silva SP. The tadpole of *Proceratophrys izecksohni* (Amphibia: Anura: Odontophrynidae). Zoologia. 2014;31:181–94.
14. Haas A. Mandibular arch musculature of anuran tadpoles, with comments on homologies of amphibian jaw muscles. J Morphol. 2001;247:1–33.
15. Inger RF. The development of a phylogeny of frogs. Evolution. 1967;21:369–84.
16. Lynch J. Evolutionary relationships, osteology, and zoogeography of leptodactyloid frogs. Univ Kans Mus Nat Hist Misc Publ. 1971;53:1–238.
17. Sokol OM. The larval chondrocranium of *Pelodytes punctatus*, with a review of tadpole chondrocrania. J Morphol. 1981;169:161–83.
18. Starrett PH. Evolutionary patterns in larval morphology. In: Vial JL, editor. Evolutionary biology of the anurans: contemporary research on major problems. University of Missouri; 1973. pp. 251–71.
19. Wassersug RJ. Internal oral features of larvae from eight anuran families: functional, systematic, evolutionary, and ecological considerations. Univ Kans Mus Nat Hist Misc Publ. 1980;68:1–146.
20. Wassersug RJ, Ronald Heyer W. A survey of internal oral features of leptodactyloid larvae (Amphibia: Anura). Smithsonian Cont Zool. 1988;457:1–99.
21. Haas A. Phylogeny of frogs as inferred from primarily larval characters (Amphibia: Anura). Cladistics. 2003;19:23–89.
22. Feng YJ, Blackburn DC, Liang D, Hillis DM, Wake DB, Cannatella DC, Zhang P. Phylogenomics reveals rapid, simultaneous diversification of three major clades of Gondwanan frogs at the cretaceous–paleogene boundary. Proc Natl Acad Sci USA. 2017;114:E5864–70.
23. Frost D, Grant T, Faivovich J, Bain RH, Haas A, Haddad CFB, de Sá RO, Channing A, Wilkinson M, Donnellan SC, Raxworthy CJ, Campbell JA, Blotto BL, Moler P, Drewes RC, Nassbaum RA, Lynch JD, Green DM, Wheeler WC. The amphibian tree of life. Bull Am Mus Nat Hist. 2006;297:1–291.
24. Grosjean S, Bordoloi S, Chuaynkern Y, Chakravarty P, Ohler A. When young are more conspicuous than adults: a new ranid species (Anura: Ranidae) revealed by its tadpole. Zootaxa. 2015;4058:471–98.
25. Dias PHS. The remarkable larval anatomy of *Proceratophrys minuta* Napoli, Cruz, Abreu, and Del-Grande, 2011 (Amphibia: Anura: Odontophrynidae). J Morphol. 2020;281:1086–97.
26. Gan LL, Hertwig ST, Das I, Haas A. The anatomy and structural connectivity of the abdominal sucker in the tadpoles of *Huia cavitympanum*, with comparisons to *Meristogenys jerboa* (Lissamphibia: Anura: Ranidae). J Zool Syst Evol Res. 2016;54:46–59.
27. Haas A, Hertwig S, Das I. Extreme tadpoles: the morphology of the fossorial megophryid larva, *Leptobranchella mjobergi*. Zoology. 2006;109:26–42.
28. Haas A, Pohlmeier J, McLeod DS, Kleinteich T, Hertwig ST, Das I, Buchholz DR. Extreme tadpoles II: the highly derived larval anatomy of *Occidozyga baluensis* (Boulenger, 1896), an obligate carnivorous tadpole. Zoomorphology. 2014;133:321–42.
29. Peixoto OL, Caramaschi U, Freire EMX. Two new species of *Phyllodytes* (anura: hylidae) from the state of alagoas, northeastern Brazil. Herpetologica. 2003;59:235–46.
30. Rowley JLL, Tran DTA, Le DTT, Hoang HD, Altig R. The strangest tadpole: the oophagous, tree-hole dwelling tadpole of *Rhacophorus vampyrus* (Anura: Rhacophoridae) from Vietnam. J Nat Hist. 2012;46:2969–78.
31. Vera Candiotti F, Dias PHS, Rowley JLL, Hertwig S, Haas A, Altig R. Anatomical features of the phytotelma dwelling, egg-eating, fanged tadpoles of *Rhacophorus vampyrus* (Anura: Rhacophoridae). J Morphol. 2021;282:769–78.
32. Zachariah A, Abraham RK, Das S, Jayan KC, Altig R. A detailed account of the reproductive strategy and developmental stages of *Nasikabatrachus sahyadrensis* (Anura: Nasikabatrachidae), the only extant member of an archaic frog lineage. Zootaxa. 2012;3510:53–64.
33. Dias PHS, Anganoy-Criollo M. Harlequin frog tadpoles—comparative buccopharyngeal morphology in the gastromyzophorous tadpoles of the genus *Atelopus* (Amphibia, Anura, Bufonidae), with discussion on the phylogenetic and evolutionary implication of characters. Naturwissenschaften. 2024;111:3.
34. Dias PHS, Araujo-Vieira K, Carvalho-e-Silva AMPT, Orrico VGD. Larval anatomy of *Dendropsophus decipiens* (A. Lutz 1925) (Anura: Hylidae: Dendropsophini) with considerations to larvae of this genus. PlosOne. 2019;14:e0219716.
35. Dias PHS, Anganoy-Criollo M, Rada M, Grant T. The tadpoles of the funnel-mouthed dendrobatids (Anura: Dendrobatidae: Colostethinae: *Silverstoneia*): external morphology, musculoskeletal anatomy, buccopharyngeal cavity, and new synapomorphies. J Zool Syst Evol Res. 2021;59:691–717.
36. Dias PHS, Vera Candiotti F, Sabbag AF, Colaço G, Silva HR, Haddad CFB, Carvalho-e-Silva AMPT, Grant T. Life on the edge: tadpoles of Cycloramphidae (Amphibia; Anura), anatomy, systematics, functional morphology, and comments on the evolution of semiterrestrial tadpoles. J Zool Syst Evol Res. 2021;59:1297–321.
37. Duellman WE. Hylid frogs of Middle America. Society for the Study of Amphibians and Reptiles; 2001.
38. Faivovich J. A cladistic analysis of *Scinax* (Anura: Hylidae). Cladistics. 2002;18:367–93.
39. Faivovich J, Haddad CFB, Garcia PCA, Frost DR, Campbell JA, Wheeler WC. Systematic review of the frog family Hylidae, with special reference to Hylinae: phylogenetic analysis and taxonomic revision. Bull Am Mus Nat Hist. 2005;2005:1–240.
40. Grant T, Rada M, Anganoy-Criollo M, Batista A, Dias PH, Jeckel AM, Machado DJ, Rueda-Almonacid JV. Phylogenetic systematics of Dart-Poison Frogs and their relatives revisited (Anura: Dendrobatoidea). S Am J Herptol. 2017;12:S1–90.
41. Larson PM, De Sá RO. Chondrocranial morphology of *Leptodactylus* larvae (Leptodactylidae: Leptodactylinae): its utility in phylogenetic reconstruction. J Morphol. 1998;238:287–305.
42. Pugener LA, Maglia AM, Trueb L. Revisiting the contribution of larval characters to an analysis of phylogenetic relationships of basal anurans. Zool J Linn Soc. 2003;139:129–55.
43. Rada M, Dias PHS, Pérez-Gonzalez JL, Anganoy-Criollo M, Rueda-Solano LA, Pinto-E MA, et al. The poverty of adult morphology: Bioacoustics, genetics, and internal tadpole morphology reveal a new species of glassfrog (Anura: Centrolenidae: *Ikakogi*) from the Sierra Nevada De Santa Marta, Colombia. PLoS ONE. 2019;14:e0215349.
44. Nascimento FAC, de Sá RO, Garcia PCA. Tadpole of the Amazonia frog *Edalorhina perezii* (Anura: Leptodactylidae) with description of oral internal and chondrocranial morphology. J Morphol. 2020;282:115–26.
45. Nascimento FAC, de Sá RO, Garcia PCA. Larval anatomy of monotypic painted ant nest frogs *Lithodytes lineatus* reveals putative homoplasies with the *Leptodactylus pentadactylus* group (Anura: Leptodactylidae). Zool Anz. 2021;290:135–47.
46. Vera Candiotti MF. Anatomy of anuran tadpoles from lentic water bodies: systematic relevance and correlation with feeding habits. Zootaxa. 2007;1600:1–175.

47. Vera Candiotti F, Dias PHS, Haas A. (in press). Musculoskeletal System. In Viertel B, editor. *Anuran Larvae*. Chimaira.
48. Frost DR. Amphibian species of the World: an online reference. Version 6.2 (accessed 1 April 2024). New York, USA: American Museum of Natural History; 2024. <https://amphibiansoftheworld.amnh.org/index.php>. Electronic Database accessible at.
49. Grandison AG. The occurrence of *Nectophrynoidea* (Anura, Bufonidae) in Ethiopia. A new concept of the genus with a description of a new species. *Monit Zool Ital Suppl.* 1978;11:119–72.
50. Grandison AG. Morphology and phylogenetic position of the west African *Didynamipus Sjoestedti* Andersson, 1903 (Anura, Bufonidae). *Monit Zool Ital Suppl.* 1981;15:187–215.
51. Lamotte M, Xavier F. Recherches sur le développement embryonnaire de *Nectophrynoidea occidentalis* Angel, amphibien anoure vivipare. I. Les principaux traits morphologiques et biométriques du développement. *Ann Emb Morphol.* 1972;5:315–40.
52. Liedtke HC, Wiens JJ, Gomez-Mestre I. The evolution of reproductive modes and life cycles in amphibians. *Nat Commun.* 2022;13:7039.
53. McDiarmid RW, Gorzula S. Aspects of the reproductive ecology and behavior of the Tepui toads, genus *Oreophrynella* (Anura, Bufonidae). *Copeia.* 1989;1989:445–51.
54. Pereyra MO, Vera Candiotti MF, Faivovich J, Baldo D. Egg clutch structure of *Rhinella rumbolli* (Anura: Bufonidae), a toad from the yungas of Argentina, with a review of the reproductive diversity in *Rhinella*. *Salamandra.* 2015;51:161–70.
55. Romero-Carvajal A, Negrete L, Salazar-Nicholls MJ, Vizuete K, Debut A, Dias PH, Vera Candiotti F. Direct development or endotrophic tadpole? Morphological aspects of the early ontogeny of the plump toad *Osornophryne occidentalis* (Anura: Bufonidae). *J Morphol.* 2023;284:e21582.
56. Van Bocxlaer I, Loader SP, Roelants K, Biju SD, Menegon M, Bossuyt F. Gradual adaptation toward a range-expansion phenotype initiated the global radiation of toads. *Science.* 2010;327:679–82.
57. Vera Candiotti MF, Baldo D, Grosjean S, Pereyra MO, Nori J. Global shortfalls of knowledge on anuran tadpoles. *Npj Biodivers.* 2023;2:22.
58. Wake MH. The reproductive biology of *Nectophrynoidea malcolmi* (Amphibia: Bufonidae), with comments on the evolution of reproductive modes in the genus *Nectophrynoidea*. *Copeia.* 1980;1980:193–209.
59. Oliveira FFR, Nascimento LB, Eterovick PC, Sazima I. Description of the tadpole and redescription of the advertisement call of *Physalaemus evangelistai* (Anura, Leiuperidae), with notes on its natural history. *J Herpetol.* 2013;47:539–43.
60. Aguayo R, Lavilla EO, Vera Candiotti MF, Camacho T. Living in fast-flowing water: morphology of the gastromyzophorous tadpole of the bufonid *Rhinella quechua* (R. *veraguensis* group). *J Morphol.* 2009;270:1431–42.
61. Pérez-González JL, Rada M, Vargas-Salinas F, Rueda-Solano LA. The tadpoles of two *Atelopus* species (Anura: Bufonidae) from the Sierra Nevada de Santa Marta, Colombia, with notes on their ecology and comments on the morphology of *Atelopus* larvae. *South Am J Herpetol.* 2020;15:47–62.
62. Chandramouli SR, Vasudevan K, Harikrishnan S, Dutta SK, Janani SJ, Sharma R, Das I, Aggarwal R. A new genus and species of arboreal toad with phytotelmonous larvae, from the Andaman Islands, India (Lissamphibia, Anura, Bufonidae). *Zookeys.* 2016;555:57–90.
63. Dubeux MJM, Nascimento FAC, Dias PHS. Larval morphology of *Frostius pernambucensis* (Anura): contribution of larval characters for the systematics of the family Bufonidae and evolution of endotrophic tadpoles. *Zoomorphology.* 2023. <https://doi.org/10.1007/s00435-023-00623-6>.
64. Leong TM, Teo SC. Endotrophic tadpoles of the Saint Andrew's cross toadlet, *Pelophryne signata* (Amphibia: Anura: Bufonidae) in Singapore. *Nat Singap.* 2009;2:21–5.
65. Viertel B, Channing A. The larva of *Schismaderma carens* (Smith, 1849) (Anura: Bufonidae): a redescription. *Alytes.* 2017;33:38–46.
66. Channing A, Rödel MO, Channing J. Tadpoles of Africa: the Biology and Identification of all known tadpoles in Sub-saharan Africa. Chimaira; 2012.
67. Kok PJR, MacCulloch RD, Means DB, Roelants K, Van Bocxlaer I, Bossuyt F. Low genetic diversity in tepui summit vertebrates. *Curr Biol.* 2012;22:R589–90.
68. Maguire B. On the Flora of the Guayana Highland. *Biotropica.* 1970;2:85–100.
69. Steyermark JA. Flora of the guayana highland: endemicity of the generic flora of the summits of the Venezuela tepuis. *Taxon.* 1979;28:45–54.
70. Carvalho VT, MacCulloch RD, Bonora L, Vogt RC. New species of *Stefania* (Anura: Cryptobatrachidae) from Northern Amazonas, Brazil. *J Herp.* 2010;44:229–35.
71. Fouquet A, Souza SM, Nunes PMS, Kok PJR, Curcio FF, De Carvalho CM, et al. Two new endangered species of *Anomaloglossus* (Anura: Aromobatidae) from Roraima State, northern Brazil. *Zootaxa.* 2015;3926:191–210.
72. Kok PJR. A new species of *Hypsiboas* (Amphibia: Anura: Hylidae) from Kaieteur National Park, eastern edge of the Pakaraima mountains. *Guyana Bull Inst Royal Sci Nat Belgique.* 2006;76:191–200.
73. Kok PJR. A new species of *Oreophrynella* (Anura: Bufonidae) from the Pantepui region of Guyana, with notes on *O. macconnelli* Boulenger, 1900. *Zootaxa.* 2009;2071:35–49.
74. Kok PJR. Two new charismatic *Pristimantis* species (Anura: Craugastoridae) from the tepuis of the Lost World (Pantepui region, South America). *Eur J Taxon.* 2013;60.
75. Kok PJR. Bones and all: a new critically endangered Pantepui species of *Stefania* (Anura: Hemiphraetidae) and a new osteological synapomorphy for the genus. *Zool Lett.* 2023;9:11.
76. Kok PJR. Out of sight, but not out of mind: a name for the *Stefania* (Anura: Hemiphraetidae) from the summit of Murispán-tepui (Bolívar State, Venezuela). *J Vert Biol.* 2023;72:1–16.
77. Kok PJR, Sambhu H, Roopsind I, Lenglet GL, Bourne GR. A new species of *Colostethus* (Anura: Dendrobatidae) with maternal care from Kaieteur National Park, Guyana. *Zootaxa.* 2006;1238:35–61.
78. Kok PJR, MacCulloch RD, Lathrop A, Willaert B, Bossuyt F. A new species of *Anomaloglossus* (Anura: Aromobatidae) from the Pakaraima Mountains of Guyana. *Zootaxa.* 2010;2660:18–32.
79. Kok PJR, Means DB, Bossuyt F. A new highland species of *Pristimantis* Jiménez De La Espada, 1871 (Anura: Strabomantidae) from the Pantepui region, northern South America. *Zootaxa.* 2011;2934:1–19.
80. Kok PJR, Nicolai MPJ, Lathrop A, MacCulloch RD. *Anomaloglossus meansi* sp. n., a new Pantepui species of the *Anomaloglossus beebei* group (Anura, Aromobatidae). *Zookeys.* 2018;99–116.
81. MacCulloch RD, Lathrop A, Minter LR, Khan SZ. *Otophryne* (Anura: Microhylidae) from the highlands of Guyana: redescription, vocalisations, tadpoles and new distributions. *Pap Avulsos Zool.* 2008;48:247–61.
82. Means DB, Savage JM. Three new malodorous rainfrogs of the genus *Pristimantis* (Anura: Brachycephalidae) from the Wokomung Massif in West-central Guyana, South America. *Zootaxa.* 2007;1658:39–55.
83. Means DB, Heinicke MP, Blair Hedges S, MacCulloch RD, Lathrop A. Exceptional diversity of *Pristimantis* Landfrogs (Anura: Terraranae) on the Wokomung Massif, Guyana, with descriptions of three new species. *J Vert Biol.* 2023;72:230261–26.
84. Rödder D, Jungfer K-H. A new *Pristimantis* (Anura, Strabomantidae) from Yuruani-tepui, Venezuela. *Zootaxa.* 2008;1814:58–68.
85. Rojas-Runjaic FJM, Salerno PE, Señaris JC, Pauly GB. Terraranans of the Lost World: a new species of *Pristimantis* (Amphibia, Craugastoridae) from Abakapá-tepui in the Chimantá Massif, Venezuelan Guayana, and additions to the knowledge of *P. muchimuk*. *Zootaxa.* 2013;3686:335–55.
86. MacCulloch RD, Lathrop A, Kok PJR, Minter LR, Khan SZ, Barrio-Amorós CL. A new species of *Adelophryne* (Anura: Eleutherodactylidae) from Guyana, with additional data on *A. gutturosa*. *Zootaxa.* 2008;1884:36.
87. Heinicke MP, Duellman WE, Trueb L, Means DB, MacCulloch RD, Hedges SB. A new frog family (Anura: Terrarana) from South America and an expanded direct-developing clade revealed by molecular phylogeny. *Zootaxa.* 2009;2211:1–35.
88. Pinheiro PDP, Kok PJR, Noonan BP, Means DB, Haddad CFB, Faivovich J. A new genus of Cophomantini, with comments on the taxonomic status of *Boana lilliae* (Anura: Hylidae). *Zool J Linn Soc.* 2019;185:226–45.
89. Fouquet A, Kok PJR, Recoder RS, Prates I, Camacho A, Marques-Souza S, et al. Relicts in the mist: two new frog families, genera and species highlight the role of Pantepui as a biodiversity museum throughout the Cenozoic. *Mol Phylogenet Evol.* 2024;191:107971.
90. Kok PJR. Islands in the Sky: Species Diversity, Evolutionary History, and Patterns of Endemism of the Pantepui Herpetofauna. PhD thesis, Leiden University, the Netherlands; 2013.
91. Vacher J-P, Kok PJR, Rodrigues MT, Lima A, Hrbek T, Werneck FP, Manzi S, Thébaud C, Fouquet A. Diversification of the terrestrial frog genus *Anomaloglossus* (Anura, Aromobatidae) in the Guiana Shield proceeded from highlands to lowlands, with successive loss and reacquisition of endotrophy. *Mol Phylogenet Evol.* 2024;192:108008.
92. Kok PJR, Broholm TL, Mebs D. Thriving in a hostile world: insights from the dietary strategy of two allopatric, closely related tepui summit endemic amphibians. *Ecol Evol.* 2020;11:8730–42.

93. Altig R, McDiarmid RW, Dias PHS. Bibliography for the Identification, Morphology, and Development of Amphibian Gametes and Larvae. H. Mueller-Hill, J. R. Mendelson III, Editors. Society for the Study of Amphibians and Reptiles. Electronic Document accessible at <https://ssarherps.org/publications/books-pamphlets/altig-larvae-biblio/>
94. Kok PJR, Means DB. Hiding in the mists: molecular phylogenetic position and description of a new genus and species of snake (Dipsadidae: Xenodontinae) from the remote cloud forest of the Lost World. *Zool J Linn Soc.* 2024;200:505–31.
95. Ron SR, Mueses-Cisneros JJ, Gutiérrez-Cárdenas PDA, Rojas-Rivera A, Lynch RL, Rocha CFD, Galarza G. Systematics of the endangered toad genus *Andinophryne* (Anura: Bufonidae): phylogenetic position and synonymy under the genus *Rhaebo*. *Zootaxa.* 2015;3947:347–66.
96. Pereyra MO, Blotto BL, Baldo D, Chaparro JC, Ron SR, Elias-Costa AJ, Iglesias PP, Venegas P, Thomé MTC, Ospina-Sarria JJ, Maciel NM, Rada M, Kolenc F, Borteiro C, Rivera-Correa M, Rojas-Runjaic FJM, Moravec J, De La Riva I, Wheeler WC, Castroviejo-Fisher S, Grant T, Haddad CFB, Faivovich J. Evolution in the genus *Rhinella*: a total evidence phylogenetic analysis of neotropical true toads (Anura: Bufonidae). *Bull Am Mus Nat Hist.* 2021;447:1–156.
97. Portik DM, Streicher JW, Wiens JJ. Frog phylogeny: a time-calibrated, species-level tree based on hundreds of loci and 5,242 species. *Mol Phylogenet Evol.* 2023;188:107907.
98. Katoh K, Toh H. Recent developments in the MAFFT multiple sequence alignment program. *Brief Bioinform.* 2008;9:286–98.
99. Katoh K, Rozewicki J, Yamada KD. MAFFT online service: multiple sequence alignment, interactive sequence choice and visualization. *Brief Bioinform.* 2019;20:1160–6.
100. Vaidya G, Lohman DJ, Meier R. SequenceMatrix: concatenation software for the fast assembly of multi-gene datasets with character set and codon information. *Cladistics.* 2011;27:171–80.
101. Goloboff PA, Farris JS, Nixon KC. TNT, a free program for phylogenetic analysis. *Cladistics.* 2008;24:774–86.
102. Goloboff PA, Morales ME. TNT version 1.6, with a graphical interface for MacOS and Linux, including new routines in parallel. *Cladistics.* 2023;39:144–53.
103. Goloboff PA. Analyzing large data sets in reasonable times: solutions for composite optima. *Cladistics.* 1999;15:415–28.
104. Nixon KC. The parsimony ratchet, a new method for rapid parsimony analysis. *Cladistics.* 1999;15:407–14.
105. Farris JS, Albert VA, Källersjö M, Lipscomb D, Kluge AG. Parsimony jackknifing outperforms neighbour-joining. *Cladistics.* 1996;12:99–124.
106. Goloboff PA, Farris JS, Källersjö M, Oxelman B, Ramirez MJ, Szumik CA. Improvements to resampling measures of group support. *Cladistics.* 2003;19:324–32.
107. Kalyaanamoorthy S, Minh BQ, Wong TK, Von Haeseler A, Jermini LS. ModelFinder: fast model selection for accurate phylogenetic estimates. *Nat Methods.* 2017;14:587–9.
108. Minh BQ, Schmidt HA, Chernomor O, Schrempf D, Woodhams MD, Von Haeseler A, Lanfear R. IQ-TREE 2: new models and efficient methods for phylogenetic inference in the genomic era. *Mol Biol Evol.* 2020;37(5):1530–4.
109. Hoang DT, Chernomor O, Haeseler AV, Minh BQ, Vinh LS. UFBoot2: improving the ultrafast bootstrap approximation. *Mol Biol Evol.* 2018;35:518–22.
110. Swofford DL. PAUP*. Phylogenetic analysis using parsimony (*and other methods). Version 4. Sinauer Associates; 2003.
111. Gosner KL. A simplified table for staging anuran embryos and larvae with notes on identification. *Herpetologica.* 1960;16(3):183–90.
112. Altig R, McDiarmid RW. Diversity: Familial and Generic Characterizations. In: Altig R, McDiarmid RW, editors. *Tadpoles: The Biology of Anuran Larvae.* 1999; pp. 295–337.
113. Altig R. A primer for the morphology of anuran tadpoles. *Herpetol Conserv Biol.* 2007;2:71–4.
114. Dingerkus G, Uhler LD. Enzyme clearing of alcian blue stained whole small vertebrates for demonstration of cartilage. *Stain Technol.* 1977;52:229–32.
115. Wassersug RJ. Oral morphology of anuran larvae: terminology and general description. *Occ Pap Mus Nat Hist Univ Kans.* 1976;48:1–23.
116. Metscher BD. MicroCT for comparative morphology: simple staining methods allow high-contrast 3D imaging of diverse non-mineralized animal tissues. *BMC Physiol.* 2009;9:11.
117. Wassersug RJ. A procedure for differential staining of cartilage and bone in whole formalin-fixed vertebrates. *Stain Technol.* 1976;51:131–4.
118. Fitch WM. Toward defining the course of evolution: minimum change for a specific tree topology. *Syst Biol.* 1971;20:406–16.
119. Fenolio DB, Mendelson JR III, Lamar WW. A new diagnosis and description of variation among adult *Rhinella ceratophrys* (Boulenger) (Amphibia: Bufonidae), with notes on ecology and distribution. *South Am J Herpetol.* 2012;7:9–15.
120. Hoogmoed M. On the presence of *Bufo nasicus* Werner in Guiana, with a redescription of the species on the basis of recently collected material. *Zool Meded.* 1977;51:265–75.
121. Pramuk JB. Phylogeny of South American *Bufo* (Anura: Bufonidae) inferred from combined evidence. *Zool J Linn Soc.* 2006;146:407–52.
122. Boulenger GA. LIII.—Account of the reptiles and batrachians collected by Mr. Edward Whymper in Ecuador in 1879–80. *Ann Mag Nat Hist.* 1882;9:457–67.
123. Gallardo JM. A propósito de *Bufo variegatus* (Günther), sapo del bosque húmedo antártico, y las otras especies de *Bufo* neotropicales. *Physis.* 1962;23:93–102.
124. Cei JM. *Bufo* of South America. In Blair WF, editor. *Evolution in the genus Bufo*: 1972; p 82–92.
125. Werner F. Neue reptilien und batrachier aus dem naturhistorischen museum in Brüssel. Nebst bemerkungen über einige andere arten. *Zool Anz.* 1903;26:246–53.
126. Smith HM, Laurent RF. Further notes upon the enigmatical *Bufo nasicus* Werner. *Bull Mus Royal d'Hist Natur.* 1950;26:1–3.
127. Cochran DM, Goin CJ. Frogs of Colombia. *Bull U S Natl Mus.* 1970;288:1–655.
128. Blair WF. *Evolution in the genus Bufo*. University of Texas; 1972.
129. Pyron RA, Wiens JJ. A large-scale phylogeny of Amphibia including over 2800 species, and a revised classification of extant frogs, salamanders, and caecilians. *Mol Phylogenet Evol.* 2011;61:543–83.
130. Jetz W, Pyron RA. The interplay of past diversification and evolutionary isolation with present imperilment across the amphibian tree of life. *Nat Ecol Evol.* 2018;2(5):850–8.
131. Duellman WE, Cusco, Amazonico. The lives of amphibians and reptiles in an amazonian rainforest. Comstock Publishing Associates; 2005.
132. Lips KR, Savage JM. Key to the known tadpoles (Amphibia: Anura) of Costa Rica. *Stud Neotrop Fauna Environ.* 1996;31:17–26.
133. Pramuk JB, Robertson T, Sites JW Jr, Noonan BP. Around the world in 10 million years: biogeography of the nearly cosmopolitan true toads (Anura: Bufonidae). *Glob Ecol Biogeogr.* 2008;17:72–83.
134. Gray J. A synopsis of the genera of reptiles and Amphibia, with a description of some new species. *Ann Philosoh.* 1825;10:193–217.
135. McDiarmid RW, Altig R. Description of a bufonid and two hylid tadpoles from western Ecuador. *Alytes.* 1990;8(2):51–60.
136. Lynch RL, Kohn S, Ayala-Varela F, Hamilton PS, Ron SR. Rediscovery of *Andinophryne olallai* Hoogmoed, 1985 (Anura: Bufonidae), an enigmatic and endangered Andean toad. *Amphib Reptile Conserv.* 2014;8:1–7.
137. Baldo D, Candiotti FV, Haad B, Kolenc F, Borteiro C, Pereyra MO, Zank C, Colombo P, Bornschein M, Sisa FN, Brusquetti F, Conte CE, Nogueira-Costa P, Almeida-Santos P, Pie MR. Comparative morphology of pond, stream and phytotelm-dwelling tadpoles of the South American Redbelly Toads (Anura: Bufonidae: Melanophryniscus). *Biol J Linn Soc.* 2014;112(3):417–41.
138. Vera Candiotti F, Grosso J, Pereyra MO, Haad MB, Lescano J, Siu-Ting K, Aguilar C, Baldo D. Larval anatomy of Andean toads of the *Rhinella spinulosa* group (Anura: Bufonidae). *Herpetol Monogr.* 2020;34:116–30.
139. Díaz LM, Cádiz A. Guía taxonómica de los Anfíbios de Cuba. *Abc Taxa.* 2008;4:1–294.
140. Landestoy MA, Turner DB, Marion AB, Hedges SB. A new species of Caribbean toad (Bufonidae, *Peltophryne*) from southern Hispaniola. *Zootaxa.* 2018;4403:523–39.
141. Vera Candiotti F, Haas A, Altig R, Peixoto O. Cranial anatomy of the amazing bromeliad tadpoles of *Phyllodytes gyrinaethes* (Hylidae: Lophophyllini), with comments about other gastromyzophorous larvae. *Zoomorphology.* 2017;136:61–73.
142. Phillips JR, Reissig J, Nicolau GK. Notes on lung development in South African ghost frogs (Anura: Heleophrynidae). *Afr J Herpetol.* 2023;72:81–90.
143. Phillips JR, Hewes AE, Schwenk K. The mechanics of air breathing in gray tree frog tadpoles, *Hyla versicolor* (Anura: Hylidae). *J Exp Biol.* 2020;223:jeb219311.
144. Sabbag AF, Dias PHS, Brasileiro CA, Haddad CFB, Wassersug RJ. Moving forwards, sideways and up in the air: observations on the locomotion of semiterrestrial tadpoles (Cycloramphidae). *Biol J Linn Soc.* 2022;136:92–110.
145. Rao D, Yang D. The study of early development and evolution of *Torrentophryne aspinia*. *Zool Res.* 1994;15:142–57.
146. Matsui M, Yambun P, Sudin A. Taxonomic relationships of *Ansonia anotis* Inger, Tan, and Yambun, 2001 and *Pedostibes maculatus* (Mocquard, 1890),

- with a description of a new genus (Amphibia, Bufonidae). *Zoolog Sci.* 2007;24:1159–66.
147. Meegaskumbura M, Senevirathne G, Wijayathilaka N, Jayawardena B, Bandara C, Manamendra-Arachchi K, Pethiyagoda R. The Sri Lankan torrent toads (Bufonidae: Adenominae: *Adenomus*): species boundaries assessed using multiple criteria. *Zootaxa.* 2015;3911:245–61.
 148. Biju S, Van Bocxlaer I, Giri VB, Loader SP, Bossuyt F. Two new endemic genera and a new species of toad (Anura: Bufonidae) from the western ghats of India. *BMC Res Notes.* 2009;2:241.
 149. Fei L, Changyuan Y, Jianping J. Colored Atlas of Chinese amphibians and their distributions. Sichuan Publishing House of Science & Technology; 2012.
 150. Tanaka K, Nishikawa K. Developmental stages of lotic-breeding toad, *Bufo torrenticola*, with comparison to lentic-breeding *B. japonicus formosus* (Amphibia: Anura: Bufonidae). *Curr Herpetol.* 2002;41:8–23.
 151. Haas A, Das I, Hertwig ST, Bublies P, Schulz-Schaeffer R. A guide to the tadpoles of Borneo. Tredition; 2022.
 152. Lavilla EO, De Sá R. Chondrocranium and visceral skeleton of *Atelopus tricolor* and *Atelophryniscus chrysophorus* tadpoles (Anura, Bufonidae). *Amphib-Reptil.* 2001;22:167–77.
 153. Moran NA. Adaptation and constraint in the complex life cycles of animals. *Annu Rev Ecol Syst.* 1994;25:573–600.
 154. Aguirre JD, Blows MW, Marshall DJ. The genetic covariance between life cycle stages separated by metamorphosis. *Proc Biol Sci.* 2014;281:20141091.

Publisher's note

Springer Nature remains neutral with regard to jurisdictional claims in published maps and institutional affiliations.